induced by L-BLP25 are characterized by the generation of cytotoxic T-lymphocytes capable of destroying MUC1-expressing tumor cells, the proliferation of CD4-positive T cells (10) and the production of pro-inflammatory cytokines (11).

A Phase IIb study in patients with Stage IIIB or IV NSCLC who had undergone primary chemo-and/or radiotherapy ($n = 171$) showed a trend towards longer survival with L-BLP25 plus best supportive care (BSC) vs. BSC alone [median: 17.4 vs. 13.0 months; adjusted hazard ratio (HR): 0.739, 95% CI: 0.509–1.073, $P = 0.112$], with a *post hoc* subgroup analysis ($n = 65$) suggesting greater survival benefit in patients with Stage IIIB locoregional disease (12). An updated analysis confirmed the survival benefit in this subgroup of patients (median: 30.6 months for L-BLP25 plus BSC vs. 13.3 months for BSC alone; adjusted HR: 0.548, 95% CI: 0.301–0.999) (13). In the Phase IIb study, L-BLP25 maintenance therapy was associated with minimal toxicity (12). Grade 1 flu-like symptoms were the most common adverse event (AE) related to the study drug (12). These safety findings were supported by a subgroup analysis of 16 patients who received L-BLP25 for at least 2 years (14).

Previous studies of L-BLP25 recruited predominantly Caucasian patients; L-BLP25 has not been studied in Japanese populations. This open-label, non-randomized Phase I study combined with a double-blind, randomized, placebo-controlled Phase II study is being conducted in Japanese patients with unresectable Stage III NSCLC after primary chemoradiotherapy. Preliminary Phase I safety data are reported.

PATIENTS AND METHODS

Study Objectives

The primary objective of the Phase I component of this combined Phase I/II study was to establish the safety of L-BLP25 1000 μg in Japanese patients with unresectable Stage III NSCLC after primary chemoradiotherapy.

Study Design

This was an open-label, non-randomized Phase I study (Study EMR: 63325–009) conducted at four centers in Japan, as part of a larger study that includes a Phase II placebo-controlled trial. This study was conducted in accordance with the Declaration of Helsinki and in compliance with Good Clinical Practice. The protocol was approved by institutional review boards and by the relevant authorities, in accordance with Japanese regulations.

Study Treatments

L-BLP25 is a lyophilized preparation consisting of BLP25 lipopeptide, immunoadjuvant monophosphoryl lipid A and three lipids (cholesterol, dimyristoyl phosphatidylglycerol and dipalmitoyl phosphatidylcholine) forming a liposomal product. Patients received subcutaneous injections of L-BLP25 1000 μg (as measured by antigen mass) once weekly for 8 weeks, followed by a 1000 μg maintenance dose every 6 weeks until disease progression [according to Response Evaluation Criteria In Solid Tumors (RECIST)] or discontinuation. L-BLP25 was supplied as a sterile lyophilized preparation that was reconstituted with 0.9% sodium chloride. The 1000 μg dose consisted of four subcutaneous injections, each containing a quarter of the total dose, administered in the deltoid or triceps region of the upper arms, and the left and right anterolateral aspects of the abdomen.

Cyclophosphamide 300 mg/m^2 i.v. single dose (maximum 600 mg) was administered 3 days before the first vaccination in order to overcome the immune suppression seen in patients with cancer, thus enhancing the effect of immunotherapy (15,16).

Patients

All patients provided written informed consent. Patients were aged ≥20 years with histologically or cytologically documented unresectable Stage III NSCLC. Inclusion criteria also required: documented stable disease or objective response (according to the RECIST criteria) after primary chemoradiotherapy (either concomitant or sequential) within 4 weeks before study entry (date of eligibility); primary thoracic chemoradiotherapy (two or more cycles of platinum-based chemotherapy, minimum radiation dose: ≥50 Gy) completed 4–12 weeks before study entry and Eastern Cooperative Oncology Group (ECOG) performance status 0–1.

Exclusion criteria included lung-cancer-specific therapy other than primary chemoradiotherapy; immunotherapy within 4 weeks prior to study entry; malignant pleural or pericardial effusion; any history of neoplasm other than lung carcinoma; autoimmune disease; immunodeficiency disease; splenectomy; and infectious conditions that could, in the investigator's opinion, compromise the patient's ability to mount an immune response.

Assessments

Safety assessments included drug exposure; incidence and type of AEs and laboratory variables. Serum cytokines [interleukin 1β (IL-1β), IL-6, IL-8 and tumor necrosis factor alpha (TNFα)] and soluble IL-2 receptor alpha (sIL-2 Rα) were measured at a central laboratory. Cytokine levels were evaluated at the pretreatment evaluation visit (within 2 weeks of study entry) and at week 5.

Analysis

An independent safety monitoring board reviewed safety data after six patients had received at least four doses of L-BLP25, which corresponded to the clinical data cut-off

date 12 June 2009. All six patients were included in the safety analysis. Descriptive statistics on incidences of AE and serum cytokine monitoring are presented.

RESULTS

Patient Characteristics and Drug Exposure

Between 11 December 2008 and 10 May 2009, eight patients were screened at four study sites. Six received L-BLP25 and were included in the safety population. Median (range) age was 63.5 (59–69) years and five were male. ECOG performance status was 0 in five patients and 1 in one patient. At first diagnosis, five had Stage IIIA disease and one had Stage IIIB disease. Four patients were diagnosed with adenocarcinoma and two with squamous cell carcinoma. The median (range) duration of NSCLC (from diagnosis) was 5.7 (4.4–9.4) months. Primary chemoradiotherapy was concomitant in four patients and sequential in two, and resulted in stable disease in one patient and objective responses (partial or complete) in five.

As of 12 June 2009, median (range) duration of treatment (L-BLP25 including cyclophosphamide) was 7.7 (4.4–13.6) weeks, with a median (range) of 8 (5–9) L-BLP25 vaccinations. The median (range) total dose of cyclophosphamide was 300.0 (299.4–300.0) mg/m^2.

Safety

Of the six patients, five (83.3%) reported at least one AE (Table 1), all of which were Grade 1. No serious AEs were observed. No AEs led to discontinuation. One patient discontinued because of disease progression.

AEs related to L-BLP25 treatment were myalgia and arthralgia in one patient, and nausea in another. AEs related to cyclophosphamide were dysgeusia in one patient, and anorexia and nausea in another.

No safety concerns were identified via serum cytokine monitoring (Fig. 1). Serum concentrations of IL-1β, sIL-2 Rα, IL-6, IL-8 and TNFα all fell within the normal range at baseline and during the study, except for two patients: one whose IL-6 levels normalized during treatment, from 12.8 (pre-treatment) to 11.3 pg/ml (normal range: 0.0–11.8 pg/ml), and another whose TNFα level increased from <2.2 (pre-treatment) to 44.49 pg/ml during treatment (normal range: 0.00–7.46 pg/ml). There were no clinically significant changes in other laboratory variables.

Table 1. Summary of adverse events (safety population)

(MedDRA preferred term)	Number of patients[a] ($n = 6$)	Related to cyclophosphamide	Related to L-BLP25
Anorexia	1	Yes	No
Arthralgia	1	No	Yes
Atrioventricular block	1	No	No
Back pain	1	No	No
Dysgeusia	1	Yes	No
Hyperuricemia	1	No	No
Injection site hematoma	1	No	No
Insomnia	1	No	No
Joint effusion	1	No	No
Myalgia	1	No	Yes
Nausea[b]	1	Yes	Yes
Radiation pneumonitis	2	No	No

L-BLP25, BLP25 liposome vaccine.
[a]Some patients experienced more than one adverse event.
[b]Experienced in the same patient on two separate occasions: the first event was considered to be related to cyclophosphamide and the second related to L-BLP25 treatment.

DISCUSSION

Preliminary safety data reported here, in six Japanese patients with unresectable Stage III NSCLC after primary chemoradiotherapy, suggest that L-BLP25 has an acceptable safety and tolerability profile in this patient population. These results were in accordance with previous findings in predominantly Caucasian populations (12,17). In a previous Phase IIb study of Caucasian patients with Stage IIIB or IV NSCLC, L-BLP25 was well tolerated with no unexpected safety issues. The most common side effects attributable to the vaccine were mild flu-like symptoms and mild injection site reactions (12). Follow-up of a subgroup of patients for ≥2 years showed that the good safety profile of L-BLP25 was maintained with prolonged treatment (14).

In March 2010 clinical trials of L-BLP25 were temporarily put on hold after a case of encephalitis occurred in a study of L-BLP25 for treatment of multiple myeloma. Subsequent work-up for the patient and overall safety analysis of L-BLP25 in NSCLC led to a lift of the clinical hold in June 2010. Trials of L-BLP25 in NSCLC restarted shortly afterwards. The data we present here were collected prior to, and so were not impacted by, the clinical hold.

Serum concentrations of pro-inflammatory cytokines were assessed in this study, in the expectation that according to its proposed mode of action, L-BLP25 induces an inflammatory and a T cell-driven immune response directed against the tumor. sIL-2 Rα is a cytokine receptor produced by activated T cells, while all other measured cytokines relate to inflammatory cells. All cytokines remained within the normal range for the majority of patients in this study, and these results did not indicate any safety concerns for L-BLP25.

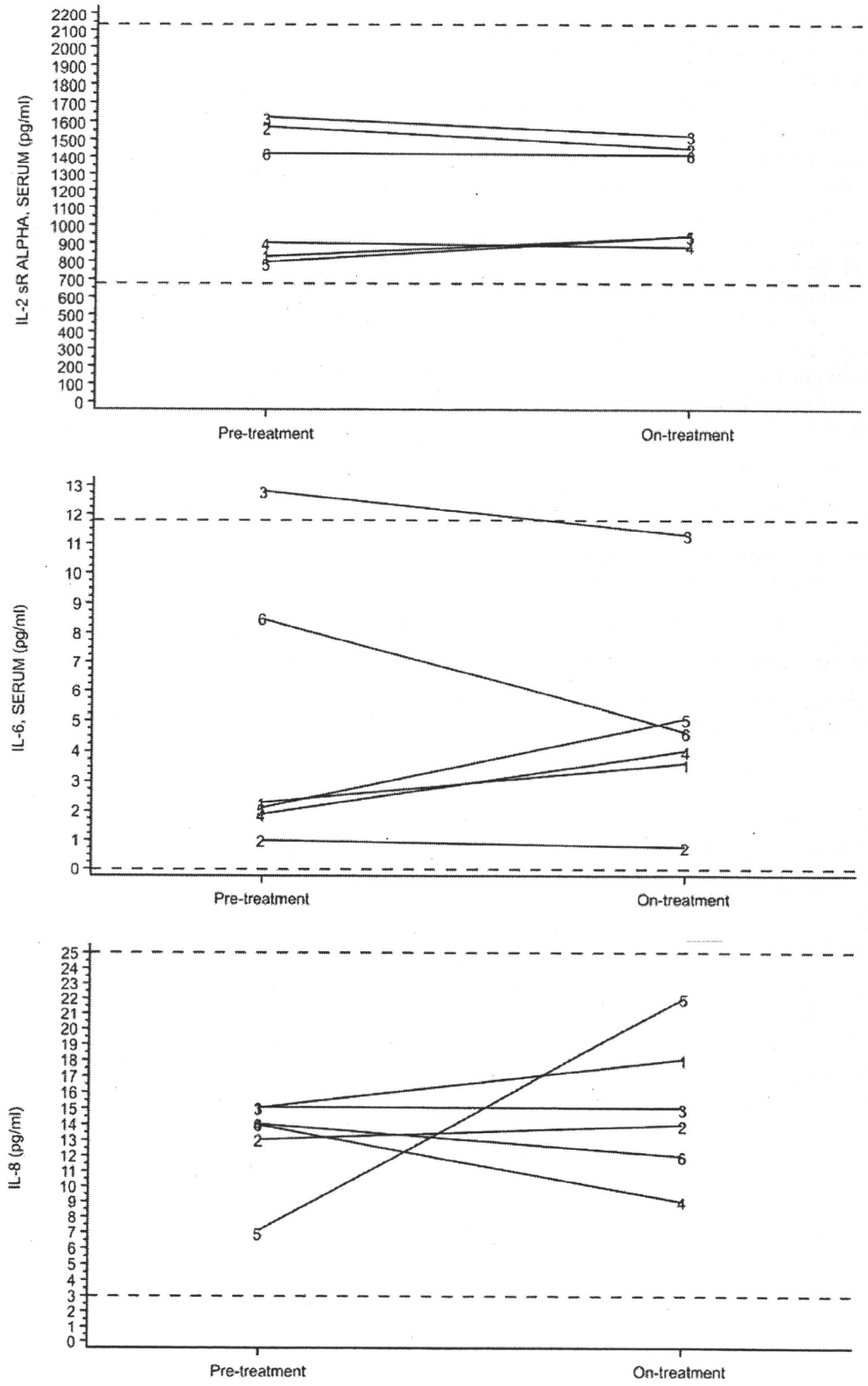

Figure 1. Serum concentrations of soluble interleukin (IL)-2 receptor alpha (sIL-2 Rα), IL-6 and IL-8 at the pretreatment evaluation visit and at week 5 of the open-label BLP25 liposome vaccine treatment period. Data not shown for serum concentrations of IL-1β (as all measurements were below the detection limit), or tumor necrosis factor alpha (as several measurements were below the detection limit). Dashed lines denote the corresponding normal ranges.

Based on these Phase I findings, the Independent Safety Monitoring Board has recommended initiation of the Phase II Stage of this combined Phase I/II study without restrictions. In the Phase II component, 168 Japanese patients with unresectable Stage III NSCLC after primary chemoradiotherapy will be randomized 2:1 to treatment with L-BLP25 plus BSC or placebo plus BSC, with once-weekly dosing for 8 weeks followed by maintenance doses every 6 weeks until disease progression or discontinuation (18). The primary objective of the Phase II stage is to compare overall survival time in the two treatment arms.

In conclusion, the first evaluation of L-BLP25 in Japanese patients with unresectable Stage III NSCLC after primary chemotherapy shows that it is well tolerated, and the safety profile is consistent with that seen in previous studies of Caucasian patients.

Funding

Editorial assistance was funded by Merck KGaA. This work was supported by Merck Serono Co. Ltd., Tokyo, Japan.

Conflict of interest statement

S. Senger is employed by Merck KGaA and holds stock in Merck KGaA. N. Morsli is employed by Merck KGaA.

References

1. Jemal A, Siegel R, Ward E, Hao Y, Xu J, Murray T, et al. Cancer statistics, 2008. *CA Cancer J Clin* 2008;58:71–96.
2. Toyoda Y, Nakayama T, Ioka A, Tsukuma H. Trends in lung cancer incidence by histological type in Osaka, Japan. *Jpn J Clin Oncol* 2008;38:534–9.
3. D'Addario G, Felip E. Non-small-cell lung cancer: ESMO clinical recommendations for diagnosis, treatment and follow-up. *Ann Oncol* 2009;20(Suppl. 4):68–70.
4. Ettinger DS, Bepler G, Bueno R, Chang A, Chang JY, Chirieac LR, et al. Non-small cell lung cancer clinical practice guidelines in oncology. *J Natl Compr Canc Netw* 2006;4:548–82.
5. Okamoto I. Overview of chemoradiation clinical trials for locally advanced non-small cell lung cancer in Japan. *Int J Clin Oncol* 2008;13:112–6.
6. Furuse K, Fukuoka M, Kawahara M, Nishikawa H, Takada Y, Kudoh S, et al. Phase III study of concurrent versus sequential thoracic radiotherapy in combination with mitomycin, vindesine, and cisplatin in unresectable stage III non-small-cell lung cancer. *J Clin Oncol* 1999;17:2692–9.
7. Giarelli E. Cancer vaccines: a new frontier in prevention and treatment. *Oncology (Williston Park)* 2007;21:11–7.
8. Ho SB, Niehans GA, Lyftogt C, Yan PS, Cherwitz DL, Gum ET, et al. Heterogeneity of mucin gene expression in normal and neoplastic tissues. *Cancer Res* 1993;53:641–51.
9. Zotter S, Hageman PC, Lossnitzer A, van den Tweel J, Hilkens J, Mooi WJ, et al. Monoclonal antibodies to epithelial sialomucins recognize epitopes at different cellular sites in adenolymphomas of the parotid gland. *Int J Cancer Suppl* 1988;3:38–44.
10. Agrawal B, Krantz MJ, Reddish MA, Longenecker BM. Rapid induction of primary human CD4+ and CD8+ T cell responses against cancer-associated MUC1 peptide epitopes. *Int Immunol* 1998;10:1907–16.
11. Guan HH, Budzynski W, Koganty RR, Krantz MJ, Reddish MA, Rogers JA, et al. Liposomal formulations of synthetic MUC1 peptides: effects of encapsulation versus surface display of peptides on immune responses. *Bioconjug Chem* 1998;9:451–8.
12. Butts C, Murray N, Maksymiuk A, Goss G, Marshall E, Soulieres D, et al. Randomized phase IIB trial of BLP25 liposome vaccine in stage IIIB and IV non-small-cell lung cancer. *J Clin Oncol* 2005;23:6674–81.
13. Butts C, Maksymiuk A, Goss G, Soulieres D, Marshall E, Cormier Y, et al. A multi-centre phase IIB randomized controlled study of BLP25 liposome vaccine (L-BLP25 or Stimuvax) for active specific immunotherapy of non-small cell lung cancer (NSCLC): updated survival analysis. *J Thorac Oncol* 2007;2:S332; abstract B1_01.
14. Butts C, Anderson H, Maksymiuk A, Vergidis D, Soulieres D, Cormier Y, et al. Long-term safety of BLP25 liposome vaccine (L-BLP25) in patients (pts) with stage IIIB/IV non-small cell lung cancer (NSCLC). *J Clin Oncol* 2009;27(15 Suppl):3055.
15. MacLean GD, Miles DW, Rubens RD, Reddish MA, Longenecker BM. Enhancing the effect of THERATOPE STn-KLH cancer vaccine in patients with metastatic breast cancer by pretreatment with low-dose intravenous cyclophosphamide. *J Immunother Emphasis Tumor Immunol* 1996;19:309–16.
16. MacLean GD, Reddish MA, Koganty RR, Longenecker BM. Antibodies against mucin-associated sialyl-Tn epitopes correlate with survival of metastatic adenocarcinoma patients undergoing active specific immunotherapy with synthetic STn vaccine. *J Immunother Emphasis Tumor Immunol* 1996;19:59–68.
17. Palmer M, Parker J, Modi S, Butts C, Smylie M, Meikle A, et al. Phase I study of the BLP25 (MUC1 peptide) liposomal vaccine for active specific immunotherapy in stage IIIB/IV non-small-cell lung cancer. *Clin Lung Cancer* 2001;3:49–57.
18. *Study of EMD531444 in Subjects with Stage III Unresectable Non-small Cell Lung Cancer (NSCLC) Following Primary Chemoradiotherapy*. Tokyo, Japan: Merck Serono Co. Ltd. http://clinicaltrials.gov/ct2/show/NCT00960115.

Biochemical and Biophysical Research Communications 407 (2011) 219–224

Contents lists available at ScienceDirect

Biochemical and Biophysical Research Communications

journal homepage: www.elsevier.com/locate/ybbrc

Switching addictions between HER2 and FGFR2 in HER2-positive breast tumor cells: FGFR2 as a potential target for salvage after lapatinib failure

Koichi Azuma [a], Junji Tsurutani [a,*], Kazuko Sakai [b], Hiroyasu Kaneda [b], Yasuhito Fujisaka [a], Masayuki Takeda [a], Masahiro Watatani [c], Tokuzo Arao [b], Taroh Satoh [a], Isamu Okamoto [a], Takayasu Kurata [a], Kazuto Nishio [b], Kazuhiko Nakagawa [a]

[a] Department of Medical Oncology, Kinki University Faculty of Medicine, 377-2 Ohnohigashi, Osakasayama, Osaka 589-8511, Japan
[b] Department of Genome Biology, Kinki University Faculty of Medicine, 377-2 Ohnohigashi, Osakasayama, Osaka 589-8511, Japan
[c] Department of Surgery, Kinki University Faculty of Medicine, 377-2 Ohnohigashi, Osakasayama, Osaka 589-8511, Japan

ARTICLE INFO

Article history:
Received 27 February 2011
Available online 4 March 2011

Keywords:
FGFR2
HER2
Lapatinib
Drug resistance
Breast cancer

ABSTRACT

Agents that target HER2 have improved the prognosis of patients with *HER2*-amplified breast cancers. However, patients who initially respond to such targeted therapy eventually develop resistance to the treatment. We have established a line of lapatinib-resistant breast cancer cells (UACC812/LR) by chronic exposure of *HER2*-amplified and lapatinib-sensitive UACC812 cells to the drug. The mechanism by which UACC812/LR acquired resistance to lapatinib was explored using comprehensive gene hybridization. The *FGFR2* gene in UACC812/LR was highly amplified, accompanied by overexpression of FGFR2 and reduced expression of HER2, and a cell proliferation assay showed that the IC_{50} of PD173074, a small-molecule inhibitor of FGFR tyrosine kinase, was 10,000 times lower in UACC812/LR than in the parent cells. PD173074 decreased the phosphorylation of FGFR2 and substantially induced apoptosis in UACC812/LR, but not in the parent cells. FGFR2 appeared to be a pivotal molecule for the survival of UACC812/LR as they became independent of the HER2 pathway, suggesting that a switch of addiction from the HER2 to the FGFR2 pathway enabled cancer cells to become resistant to HER2-targeted therapy. The present study is the first to implicate FGFR in the development of resistance to lapatinib in cancer, and suggests that FGFR-targeted therapy might become a promising salvage strategy after lapatinib failure in patients with HER2-positive breast cancer.

1. Introduction

Breast cancer is the second most frequent malignancy worldwide, and the prognosis of patients with metastatic disease still remains very poor, despite intensive research and drug development [1]. Amplification of the human epidermal growth factor receptor 2 (HER2) gene has been detected in 20–30% of human breast cancers, driving tumor development and being associated with a poor outcome [2]. HER2 forms dimers to become active, and its dimerization partners are the epidermal growth factor receptor (EGFR), HER2 itself, and HER3 in most cases. Since EGFR is a molecule frequently expressed in HER2-positive breast cancer, interaction between EGFR and HER2 could be important for the maintenance of oncogenesis [3]. Thus, targeting HER2 and EGFR together appears to be a promising therapeutic strategy for patients with *HER2*-amplified breast cancer, and multi-targeted small-molecule inhibitors such as lapatinib, BIBW2992 and AZD8931, directed against EGFR family members, have been developed for this purpose. Lapatinib binds to the ATP binding sites of EGFR and HER2, thus inhibiting their tyrosine kinase activity [4].

Acquired resistance to HER2-targeted drugs is one of the major obstacles to further improvement of clinical outcomes in this field, and research efforts have been focused on clarifying the mechanisms by which cancer cells acquire resistance to lapatinib. Several mechanisms of resistance to trastuzumab, a humanized monoclonal antibody against HER2, have been proposed, such as the presence of a truncated form of HER2 without an extracellular domain, loss of PTEN, and *PIK3CA* mutations in pre-clinical models, and such mechanisms may also have some implications for the lapatinib resistance phenotype [5–7]. In addition, overexpression of AXL, a receptor type kinase, has been reported to be a critical player for bypassing lapatinib-elicited HER2-PI3K-Akt signaling and conferring resistance to the drug in a breast cancer cell line [8].

Abbreviations: FGFR2, fibroblast growth factor receptor 2; HER2, human epidermal growth factor receptor 2; TKI, tyrosine kinase inhibitor; EGFR, epidermal growth factor receptor; IC_{50}, median inhibitory concentration; siRNA, small interfering RNA; Erk, extracellular signal-regulated kinase; RNAi, RNA interference; CGH, comprehensive gene hybridization.

* Corresponding author.
E-mail address: tsurutani_j@dotd.med.kindai.ac.jp (J. Tsurutani).

0006-291X/$ - see front matter © 2011 Elsevier Inc. All rights reserved.
doi:10.1016/j.bbrc.2011.03.002

Fibroblast growth factor receptor 2 (FGFR2) is a member of the FGFR tyrosine kinase family, and consists of 4 receptors and 23 ligands [9]. Ligand binding leads to FGFR2 dimerization, autophosphorylation, and activation of signaling components including Akt and Erk kinases. Amplification and overexpression of the *FGFR2* gene is observed in gastric cancer and breast cancer [9], and single-nucleotide polymorphisms (SNPs) of the *FGFR2* gene are associated with a higher risk of sporadic breast cancer [10]. These features suggest that *FGFR2* may have an oncogene-like character, and be capable of transforming normal cells. This gene could act as a driving force for transformation of cancer cells into a further malignant phenotype, and constitute a potential target of treatment in cancer patients whose tumors express the protein.

Here we report that subpopulations of cells with *FGFR* gene amplification play a pivotal role in development of resistance to lapatinib in HER2-positive breast cancer.

2. Materials and methods

2.1. Cell culture and reagents

A human breast cancer cell line, UACC812 was obtained from the American Type Culture Collection (Manassas, VA), and cultured under a humidified atmosphere of 5% CO_2 at 37 °C in RPMI 1640 medium (Sigma, St. Louis, MO) supplemented with 10% fetal bovine serum. Gefitinib was obtained from Kemprotec Ltd. (UK). Lapatinib was obtained from Chemietek (Indianapolis, IN). PD173074 was purchased from Sigma (St. Louis, MO).

2.2. Generation of a lapatinib-resistant line and floating line from UACC812

The UACC812 cells were grown initially in medium containing 0.01 μM lapatinib, and the concentration was gradually increased up to 1 μM over the following 8 months to establish lapatinib-resistant cell lines (UACC812/LR).

2.3. Array-based comparative genomic hybridization

The Genome-wide Human SNP Array 6.0 (Affymetrix, Santa Clara, CA) was used to perform array-CGH on genomic DNA from each of the cell lines, in accordance with the manufacturer's instructions. A total of 250 ng of genomic DNA was digested with the restriction enzymes Nsp I and Sty I in independent parallel reactions (SNP6.0), ligated to the adaptor, and amplified using PCR with a universal primer and TITANIUM Taq DNA Polymerase (Clontech). The PCR products were quantified, fragmented, end-labeled, and hybridized onto a Genome-wide Human SNP Array 6.0. After washing and staining in Fluidics Station 450 (Affymetrix), the arrays were scanned to generate CEL files using the GeneArray Scanner 3000 and GeneChip Operating Software ver.1.4. In the array-CGH analysis, sample-specific changes in copy number were analyzed using Partek Genomic Suite 6.4 software (Partek Inc., St. Louis, MO).

2.4. Growth assay in vitro

Cells were cultured in 96-well flat-bottomed plates for 24 h before exposure to various concentrations of drugs for 72 h. TetraColor One (5 mM tetrazolium monosodium salt and 0.2 mM 1-methoxy-5-methyl phenazinium methylsulfate; Seikagaku, Tokyo, Japan) was then added to each well, and the cells were incubated for 3 h at 37 °C before measurement of absorbance at 490 nm with a Multiskan Spectrum instrument (Thermo Labsystems, Boston, MA). Absorbance values were expressed as a percentage relative to untreated cells, and the concentration of tested drugs resulting in 50% growth inhibition (IC_{50}) was calculated using the Prism program (GraphPad, San Diego, CA).

2.5. Cell death assay

After incubation, cells were harvested by trypsinization and resuspended in a solution of 1 μg/mL propidium iodide in PBS, then immediately acquired on the FL3 channel of a flow cytometer. The population of propidium iodide-positive cells was considered dead, whereas the propidium iodide-negative population was considered viable.

2.6. Immunoblot analysis

Cells were washed twice with ice-cold PBS and then lysed with 1× Cell Lysis Buffer (Cell Signaling Technology) containing 20 mM Tris–HCl (pH 7.5), 150 mM NaCl, 1 mM EDTA, 1% Triton X-100, 2.5 mM sodium pyrophosphate, 1 mM phenylmethylsulfonyl fluoride, and leupeptin (1 μg/ml). The protein concentration of cell lysates was determined with a BCA protein assay kit (Thermo Fisher Scientific), and equal amounts of protein were subjected to SDS–PAGE on a 4–12% gradient gel. The separated proteins were transferred to a PVDF membrane, which was then incubated with Blocking One solution (Nakarai Tesque, Kyoto, Japan) for 20 min at room temperature before incubation overnight at 4 °C with primary antibodies, including those against phosphorylated FGFR, phosphorylated EGFR(Y1086), phosphorylated HER2(Y1221/1222), EGFR, FGFR1, FGFR3, FGFR4, phosphorylated AKT, AKT, ERK, PARP, caspase-3 (Cell Signaling Technology, Danvers, MA), HER2 (Millipore), FGFR2 (Bek) and phosphorylated ERK (Santa Cruz Biotechnology) or β-actin (1:5000 dilution, Sigma). The membrane was then washed with PBS containing 0.05% Tween 20 before incubation for 1 h at room temperature with horseradish peroxidase-conjugated antibody against rabbit immunoglobulin G (Sigma). Immune complexes were finally detected using ECL Western blotting detection reagents (GE Healthcare, Little Chalfont, UK). The RTK array was purchased from R & D Systems (Minneapolis, MN) and used in accordance with the manufacturer's instructions.

2.7. Assay of phospho-FGFR2 activity

The activity of p-FGFR2 in cell lysates was measured using ELISA in accordance with the manufacturer's procedures (Human phosphor-FGFR2 Duoset; R & D Systems). The lysates were prepared as described above. All samples were run in triplicate assays. Color intensity was measured at 450 nm using a spectrophotometric plate reader. Growth factor concentrations were determined by comparison with standard curves.

2.8. FGFR2 gene silencing using small interfering RNA

Cells were plated at 50–60% confluence in six-well plates or 25 cm^2 flasks and then incubated for 24 h before transient transfection for 48 h with small interfering RNAs (siRNAs) mixed with Lipofectamine reagent (Invitrogen, Carlsbad, CA). A siRNA specific for FGFR2 mRNA and a nonspecific siRNA (control) were obtained from Nippon EGT (Toyama, Japan). The cells were then subjected to flow cytometry and immunoblot analysis.

2.9. Immunohistochemistry (IHC)

Paraffin-embedded tissue samples were cut at a thickness of 4 μM and examined on coated glass slides, after labeling with antibodies directed against the following using the ChemMate ENVISION method (DakoCytomation, Glostrup, Denmark). Endogenous

peroxidase activity was inhibited by incubating the slides in 3% H_2O_2 for 20 min. FGFR2 (C-17, Santa Cruz Biotechnology) antigen retrieval was done by microwaving for 10 min in Target Citrate Solution (pH 6.0). Each slide was incubated overnight with the antibody at 4 °C. For staining detection, the ChemMate ENVISION method was used with DAB as the chromogen. The expression of FGFR2 protein in the cell membrane and cytoplasm was investigated in detail. FGFR2 expression was classified into three categories: score 0, no staining at all; or membrane expression in <10% of cancer cells; score 1+, faint/barely perceptible partial membrane expression in ⩾10% of cancer cells; score 2+, weak to moderate expression on the entire membrane in ⩾10% of the cancer cells; score 3+, strong expression on the entire membrane in ⩾10% of cancer cells. All IHC studies were evaluated by two IHC-experienced reviewers (K.A. and J.T.) who were blind to the conditions of the patients. Consistent results were obtained in 14 out of 16 samples, and two IHC samples without consistency were subjected to scoring by a third reviewer who was also blinded to the clinical information and scores assigned previously by the other two reviewers. Then, the majority scores were employed as the final results.

2.10. Study population and survival analysis

All patients received lapatinib between 2009 and 2010 at Kinki University School of Medicine. Sixteen tumors from a series of 13 patients diagnosed as having HER2-positive metastatic breast cancer were collected from the files of the Pathology Department, Kinki University School of Medicine, covering the period between 2009 and 2010. The HER2 status was considered positive if the local institution reported grade 3+ staining intensity (on a scale of 0–3) by means of IHC analysis or grade 2+ staining intensity by means of IHC analysis with gene amplification on fluorescence in situ hybridization. Details of the patients' clinical characteristics, including age, hormone status, prior therapy, and tumor response were obtained from chart review by an independent reviewer who was unaware of the results of IHC analysis. Tumor responses were evaluated after chemotherapy according to the Response Evaluation Criteria for Solid Tumors (RECIST). Four sites of metastasis were included. Any material that had been poorly fixed and/or had low cellularity was rejected. Paraffin-embedded tissues were obtained, and histologic examination of slides stained with hematoxylin-eosin and saffron was carried out by a specialist. All patients provided written informed consent for collection of their tissue material and clinical data for research purposes, and the tissue procurement protocol was approved by the institutional review board.

Progression-free survival was defined as the time between the onset of chemotherapy and the date when disease progression began. Patients without progression were regarded as censored at the date of the last follow-up. Curves for progression-free survival were estimated by the Kaplan–Meier method, and differences in survival functions were compared by the log-rank test.

All tests were two-sided, and differences at $P < 0.05$ were considered statistically significant. All the statistical analyses were conducted using JMP version 8 software (SAS Institute Inc., Cary, NC).

2.11. Fluorescence in situ hybridization

The gene copy number per cell for *HER2* was determined by fluorescence in situ hybridization (FISH) with the use of *HER2/neu* (17q11.2–q12) Spectrum Orange and CEP17 (chromosome 17 centromere) Spectrum Green probes (Vysis; Abbott, Des Plaines, IL). Gene amplification was defined as a mean *HER2*/chromosome 17 copy number ratio of >2.

2.12. Statistics

Experimental values were expressed ±SE. Statistical comparison of mean values was done using Student's *t* test.

3. Results

3.1. Establishment of lapatinib-resistant breast cancer cells

The UACC812 cells were grown initially in medium containing 0.01 μM lapatinib, and the concentration was gradually increased to 1 μM over the following 8 months to establish lapatinib-resistant cell lines (UACC812/LR). Cell growth assays were performed for the UACC812 cells and the UACC812/LR cells with various doses of lapatinib and gefitinib, as indicated in Fig. 1A, and the IC_{50} values were determined (Fig. 1A inset). UACC812/LR cells were resistant to lapatinib and gefinitib in comparison with the parent cells, the IC_{50} values for lapatinib (4.2433 ± 0.5066 μM) and gefitinib (11.1300 ± 0.5474 μM) being 42 times and 6 times higher than those in UACC812 (0.1006 ± 0.0053 μM and 1.9223 ± 0.3744 μM), respectively, but no differences were seen between the two cell lines in terms of the IC_{50} values for cisplatin and 5-FU (Fig. 1A inset), suggesting that chronic exposure of the UACC812 cells to lapatinib had induced resistance specific to EGFR or HER2 inhibitors.

3.2. FGFR2 gene amplification in UACC812/LR

To overview the chromosomal divergences between the parent cell line and its derivative, comprehensive gene hybridization (CGH) analyses were performed as described in Section 2. This revealed that the UACC812/LR cells harbored an amplification of the fibroblast growth factor receptor 2 (FGFR2) gene, the gene copy number in UACC812/LR being approximately 20 times that in UACC812 (Fig. 1B). Lysates of the parent and the derivative cells were subjected to Western blotting-based high-throughput analysis for expression of various receptor type kinases (RTK), and a dramatic increase in the expression of FGFR2 was observed in UACC812/LR relative to UACC812 (Fig. 1C). In contrast, the expression of HER2 was reduced in UACC812/LR in comparison to the parent cells (Fig. 1C upper panel). HER2-FISH analysis revealed that the *HER2* gene amplification was present in UACC812 cells, but not in UACC812/LR cells (Fig. 1C lower panel). To examine the role of FGFR2 in the growth of the parent cells and their derivative, an FGFR-TKI, PD173074, was utilized, and cell growth assays were performed for UACC812 and UACC812/LR treated with various concentrations of PD173074. UACC812/LR was more sensitive than UACC812 to PD173074, the IC_{50} (0.00121 ± 0.0034 μM) being 10,000 times lower than that for the parent cells (10.3373 ± 1.6629 μM), indicating that UACC812/LR cells had acquired dependency on the FGFR2 pathway, whereas FGFR2 played no role in the cell growth of UACC812 (Fig. 1D and inset).

3.3. UACC812/LR shows high phosphorylation of FGFG2 and undergoes apoptosis upon exposure to a FGFR tyrosine kinase inhibitor

To further evaluate the findings of the RTK arrays and cell growth assays, Western blotting was performed for biochemical profiling of these cell lines. Overexpression of phosphorylated FGFR2 (p-FGFR2) and native FGFR2, and downregulation of p-HER2 and p-EGFR in UACC812/LR cells relative to the parent cells were observed (Fig. 2A). The two cell lines were treated with lapatinib (1 μM) or PD173074 (0.1 and 1 μM) for 24 h, and the cell lysates were then subjected to Western blot analysis. The basal levels of p-EGFR, p-HER2 and native HER expression were

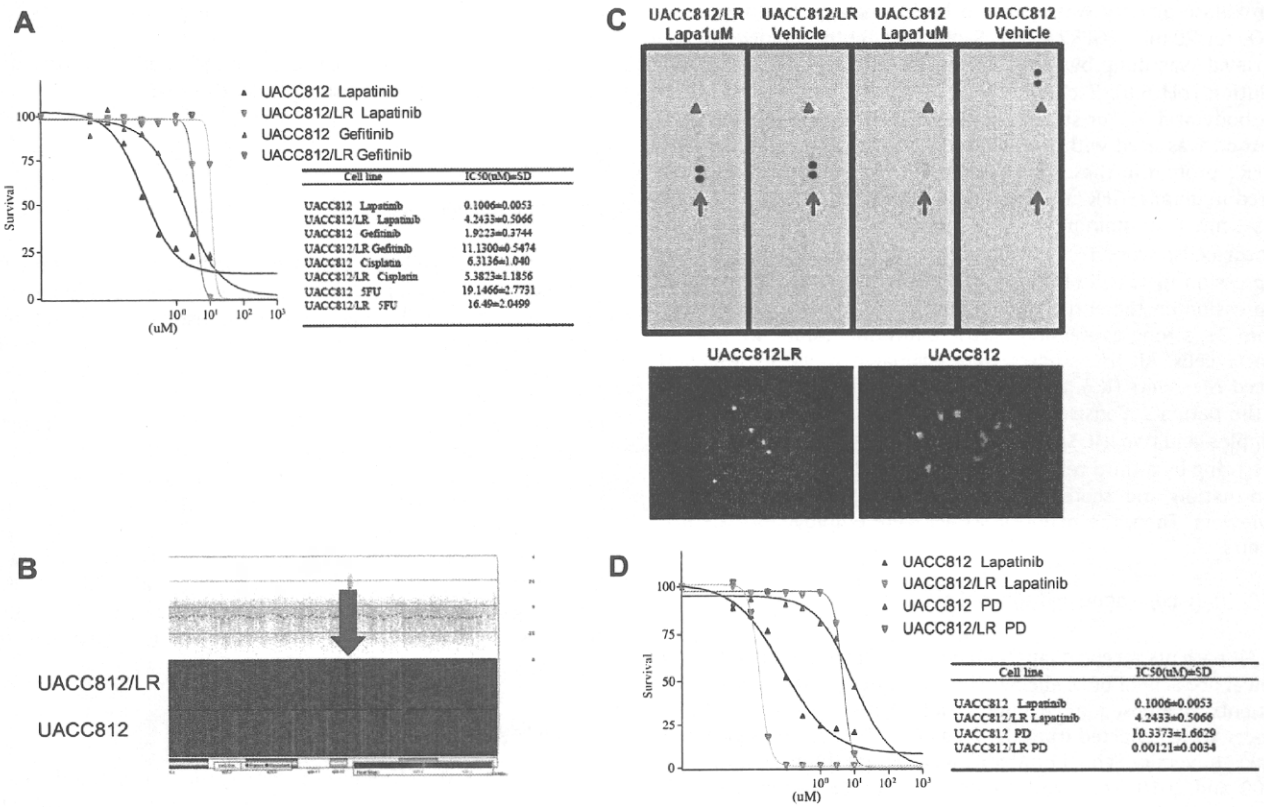

Fig. 1. Lapatinib-resistant cancer cells harbor *FGFR2* gene amplification, and are preferentially sensitive to an FGFR-TKI. (A) Cell growth assays were performed using UACC812 cells and their derivative, UACC812/LR cells, treated with lapatinib, gefitinib, cisplatin or 5-FU for 72 h, and IC_{50} values are shown in the inset. Results represent the mean ± SE of three experiments performed in triplicate. (B) *FGFR2* gene amplification detected in UACC812/LR cells. Comprehensive gene hybridization analysis revealed that the gene on chromosome 10q26 was highly amplified in UACC812/LR relative to its parent cell line. (C) Lysates from UACC812 cells and UACC812/LR cells treated with vehicle or 1 μM lapatinib for 6 h were subjected to Western blotting-based high-throughput analysis for RTKs. Arrows and arrowheads indicate signals for FGFR2 and HER2, respectively. Left column: UACC812/LR cells treated with 1 μM lapatinib; Second column from left: UACC812/LR treated with vehicle; Second column from right: UACC812 cells treated with 1 μM lapatinib; Right column: UACC812 cells treated with vehicle. Images of HER2-FISH analyses in UACC812 and UACC812/LR are shown. (D) Cell growth assays were performed using UACC812 cells and UACC812/LR cells with lapatinib or PD173074 at various doses for 72 h. IC_{50} values are shown in the inset. Results represent the mean ± SE of three experiments performed in triplicate.

decreased, and those of p-FGFR and native FGFR2 were dramatically increased in UACC812/LR cells (Fig. 2A). Lapatinib inhibited the expression of p-HER2 and p-EGFR accompanied by downregulation of p-Akt and p-Erk in UACC812 cells, but no inhibition of the phosphorylation of these signal components was observed in UACC812/LR (Fig. 2A). On the other hand, PD173074 did not affect the level of phosphorylated Akt or Erk in the parent cells, but inhibited that of p-FGFR along with p-Akt and p-Erk in UACC812/LR cells (Fig. 2A). Cleaved poly (ADP-ribose) polymerase (PARP) and caspase 3 as markers of apoptosis were increased in UACC812 and UACC812/LR after treatment with lapanib or PD173074, respectively, suggesting that the parent cells and their derivative were dependent on the different pathways for survival (Fig. 2A). Since a pan-antibody against p-FGFR was utilized in the Westen blotting to detect the pharmacological activity of PD173074, we further examined p-FGFR2 in an ELISA assay using a specific antibody against p-FGFR2 in UACC812 and UACC812/LR cells treated with lapatinib or PD173074 (Fig. 2B). We found that the basal level of p-FGFR2 was increased in UACC812/LR relative to the parent cells, and that phosphorylation was inhibited by PD173074 but not by lapatinib. Induction of cell death with lapatinib and/or pharmacological or genetic abrogation of FGFR2 was then measured in UACC812 and UACC812/LR cells (Fig. 2D). Cell death was induced in UACC812 cells treated with lapatinib but not in those treated with PD173074 (Fig. 2D left panel) or si-RNA for FGFR2 (Fig. 2D right panel). There were no increases in the percentage of cell death induced by lapatinib upon addition of PD173074 or si-RNA for FGFR2 in UACC812 cells or UACC812/LR (Fig. 2D left panel and right panel). Nonetheless, PD173074 and si-RNA for FGFR2 dramatically induced cell death in UACC812/LR cells (Fig. 2D left panel and right panel). Validation of the biochemical effects of si-RNA treatment on FGFR2 is shown in Fig. 2C. Overexpression of FGFR2 was observed in UACC812/LR cells relative to UACC812 cells, and treatment with si-RNA for FGFR2 reduced the expression of FGFR2, accompanied by inhibition of p-Akt and p-Erk in UACC812/LR cells (Fig. 2C). Cleaved PARP and caspase 3 were induced in UACC812 cells and UACC812/LR cells treated with lapatinib and/or si-RNA for FGFR2, respectively (Fig. 2C). Together, these findings suggested that UACC812/LR cells had become addicted to the FGFR2 pathway for survival in the absence of the activated HER2 pathway during the development of resistance to lapatinib.

3.4. High expression of FGFR2 in tumor specimens is associated with poor response to lapatinib

To further evaluate the role of FGFR2 in a clinical setting, we examined tissue specimens obtained from 13 consecutive patients with metastatic HER2-positive breast cancer treated with lapatinib between 2009 and 2010 at our institution. The median age of the patients was 60 years (35–69 years) and the median follow-up time after administration of lapatinib was 275 days (42–358 days). All the patients had been treated with lapatinib, and the

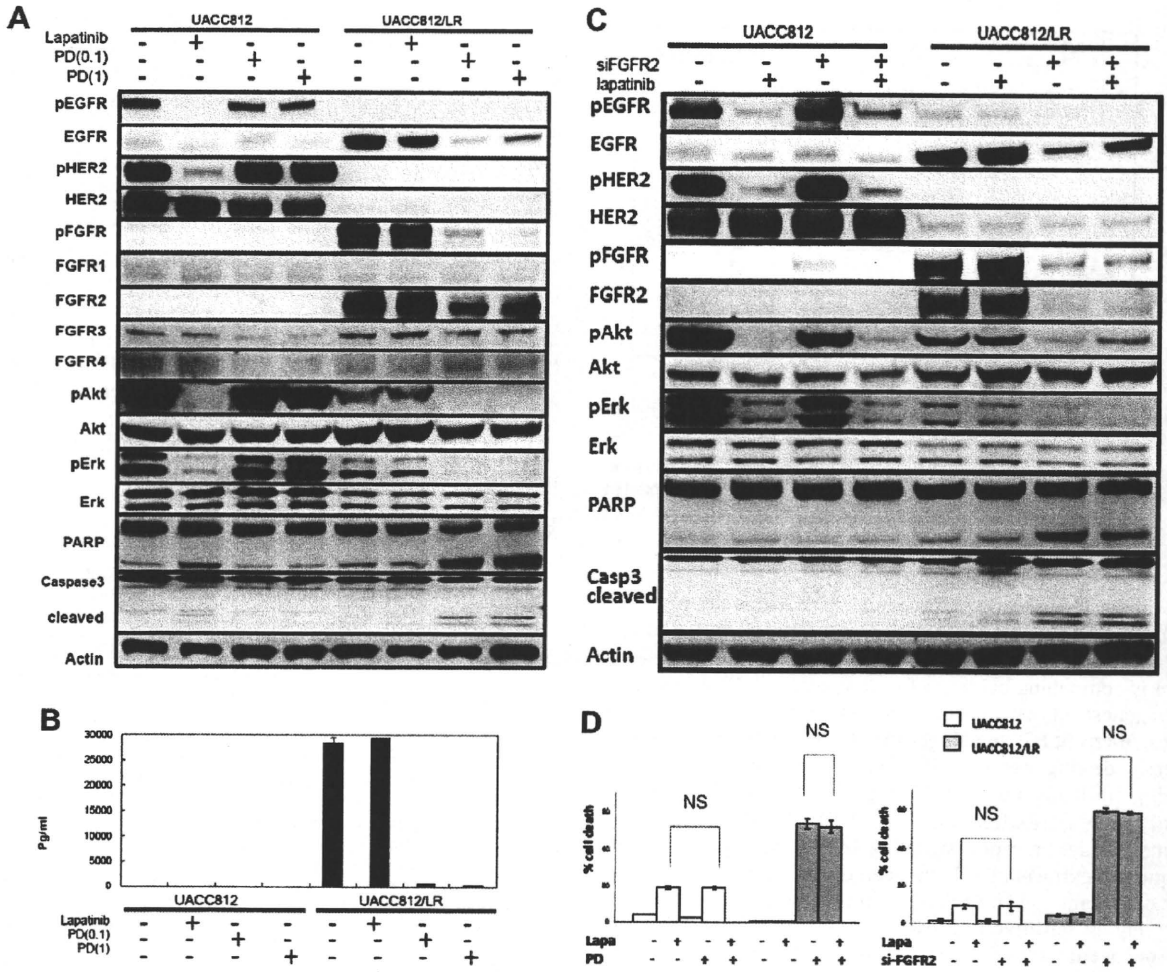

Fig. 2. FGFR2 is active in the lapatinib-resistant cell line, UACC812/LR, but not in the parental cells. (A) UACC812 cells and UACC812/LR cells were treated with 1 μM lapatinib, or 0.1 or 1 μM PD173074 for 24 h, as described in Section 2. Lysates were subjected to Western blotting with the indicated antibodies. (B) Phospho-FGFR2 levels were measured in UACC812 cells and UACC812/LR cells treated with vehicle, 1 μM lapatinib, or 0.1 or 1 μM PD173074 using an ELISA-based assay. Results represent the mean ± SE of three experiments performed in triplicate. (C) UACC812 cells and UACC812/LR cells were treated with 1 μM lapatinib and/or si-RNA for FGFR2 for 24 h after completion of transfection. Lysates were subjected to Western blotting with the indicated antibodies. (D) UACC812 cells and UACC812/LR cells were treated with 1 μM lapatinib and/or 0.1 μM PD173074 for 48 h (left panel) or with 1 μM lapatinib and/or si-RNA for FGFR2 for 48 h after completion of transfection (right panel). The cells were harvested and subjected to flow cytometry analysis to assess the extent of cell death. Results represent the mean ± SE of three experiments performed in triplicate. NS, not statistically significant.

Table 1
Clinicopathological features of HER2 positive MBC.

Patients #	Age	Primary hormone receptor status	Prior therapy	Response*	FGFR2 expression
1	52	ER+, PgR+	H, T, A	SD	0
2	53	ER+, PgR−	H, A	SD	1+
3	47	ER+, PgR−	H, T, A	PR	1+
4	60	ER+, PgR−	H, T	SD	1+
5	69	ER−, PgR−	H, T, A	PD	2+
6	67	ER−, PgR−	H	NE	1+
7	52	ER+, PgR−	H, T	PD	0
8	47	ER−, PgR−	H, T, A	SD	1+
9	35	ER+, PgR+	H , T, A	PR	1+
10	65	ER−, PgR−	H, T, A	NE	0
11	61	ER−, PgR−	H , T, A	PD	2+
12	69	ER+, PgR+	H, T, A	PD	2+
13	59	ER−, PgR−	H, T	PR	0

MBC, metastatic breast cancer; ER, estrogen receptor; PgR, progesterone receptor; CR, complete response; PR, partial response; SD, stable disease; PD, progressive disease; NE, not evaluable; H, Herceptin; T, Taxanes; A, Anthracycline.
* Response to lapatinib-containing regimens.

clinicopathological features including IHC scores of FGFR2 in tumor specimens are summarized in Table 1. Time to progression (TTP) while receiving the treatment was plotted using Kaplan–Meier curves stratified by FGFR2 expression (score 0, 1 vs. 2, 3, Fig. 3), and the patients with FGFR2-overexpressing tumors had significantly poor survival ($P = 0.0082$), suggesting that FGFR2 may play at least a partial role in the development of resistance to lapatinib, probably through selection of FGFR2-overexpressing tumor cells.

4. Discussion

Several models have been proposed to account for the clinical resistance to HER2-targeted therapies including *PIK3CA* gene mutation and *AXL gene amplification* [5–8]. Gene sequence analyses revealed that UACC812 and UACC812/LR did not harbor *PIK3CA* gene mutation (data not shown), and Western blotting showed that UACC812/LR cells do not express AXL (data not shown), indicating that these two molecules are not causative factors for acquired resistance to lapatinib in UACC812/LR. Instead, the

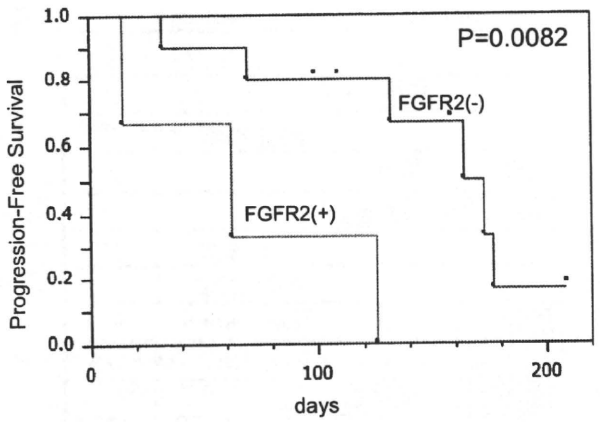

Fig. 3. Kaplan–Meier curves illustrating associations between protein expression and progression-free survival since the start of lapatinib. Survival curves are plotted as graphs according to FGFR2 expression level. The *P*-value was calculated using Log-rank test.

present model revealed amplification of *FGFR2* in lapatinib-resistant cells, and activation of FGFR2 substantially contributed to survival of the cells.

There is compelling evidence for deregulated FGF signaling in the pathogenesis of many cancers that originate from different tissue types. Aberrant FGF signaling can promote tumor development by directly driving cancer cell proliferation and survival. The underlying mechanism driving FGF signaling is largely tumor-specific, and can be attributed to genomic *FGFR* alterations that drive ligand-independent receptor signaling. Mutations of *FGFR2*, which are frequently extracellular, have been described in 12% of endometrial carcinomas [11]. *FGFR2*-mutant endometrial cancer cell lines are highly sensitive to FGFR tyrosine kinase inhibitors, suggesting oncogenic addiction of the cancer cells to the activated form of mutant FGFR [12]. In this study, gene sequencing analysis of *FGFR2* in UACC812 cells and UACC812/LR cells revealed no mutations, but gene amplification was noted in UACC812/LR in comparison with UACC812. Amplifications of *FGFR2* have been reported in approximately 10% of gastric cancers, and have been associated with poor prognosis [13]. Gastric cancer cell lines with *FGFR2* amplifications show ligand-independent signaling and are highly sensitive to FGFR inhibitors [13]. Inhibition of FGFR2 substantially induced cell death in UACC812 cells/LR harboring gene amplification of *FGFR2*, but not in UACC812 cells, and this was consistent with the above reports.

UACC812/LR cells showed loss of *HER2* amplification after chronic exposure to lapatinib, being reminiscent of clinical observations. Loss of *HER2* amplification following trastuzumab-based neoadjuvant systemic therapy has been reported in patients with residual breast cancers [14]. One third of patients with significant residual disease showed loss of *HER2* amplification, and this change was associated with poor relapse-free survival. We speculate that these residual tumors after trastuzumab-based therapy may have harbored alternative driving genes to support further tumor development under selection pressure with trastuzumab, and our model using UACC812/LR cells recapitulated the clinical loss of HER2 resulting from HER2-targeted therapies, although lapatinib was used instead of trastuzumab in this study.

Together, these findings suggest that FGFR2 may be a key molecule in the development of resistance to lapatinib in HER2-positive breast cancer through selection of cells with a growth advantage and improved survival, and that FGFR-targeted therapy may be a promising strategy for breast cancer patients in whom treatment with lapatinib has failed. Further clinical studies using a larger set of tumor specimens should be performed to confirm our findings in a small set of clinical samples, and development of FGFR-targeted therapy is warranted to clarify the role of FGFR in resistance to HER2-targeted medicines.

References

[1] J. Ferlay, H.R. Shin, F. Bray, et al., Estimates of worldwide burden of cancer in 2008, GLOBOCAN 2008, Int. Cancer. 127 (2010) 2893–2917.
[2] D.J. Slamon, G.M. Clark, S.G. Wong, et al., Human breast cancer: correlation of relapse and survival with amplification of the HER2/neu oncogene, Science 235 (1987) 177–182.
[3] M.P. DiGiovanna, D.F. Stern, S.M. Edgerton, et al., Relationship of epidermal growth factor receptor expression to ErbB-2 signaling activity and prognosis in breast cancer patients, J. Clin. Oncol. 20 (2005) 1152–1160.
[4] G.E. Konecny, M.D. Pegram, N. Venkatesan, et al., Activity of the dual kinase inhibitor lapatinib (GW572016) against HER-2-overexpressing and trastuzumab-treated breast cancer cells, Cancer Res. 66 (2006) 1630–1639.
[5] M. Scaltriti, F. Rojo, A. Ocana, et al., Expression of p95HER2, a truncated form of the HER2 receptor, and response to anti-HER2 therapies in breast cancer, J. Natl. Cancer Inst. 99 (2007) 628–638.
[6] D. Faratian, A. Goltsov, G. Lebedeva, et al., Systems biology reveals new strategies for personalizing cancer medicine and confirms the role of PTEN in resistance to trastuzumab, Cancer Res. 69 (2009) 6713–6720.
[7] P.J.A. Eichhorn, M. Gili, M. Scaltriti, et al., Phosphatidylinositol 3-kinase hyperactivation results in lapatinib resistance that is reversed by the mTOR/phosphatidylinositol 3-kinase inhibitor NVP-BEZ235, Cancer Res. 68 (2008) 9221–9230.
[8] L. Liu, J. Greger, H. Shi, et al., Novel mechanism of lapatinib resistance in HER2-positive breast tumor cells: activation of AXL, Cancer Res. 69 (2009) 6871–6878.
[9] N. Turner, R. Grose, Fibroblast growth factor signaling: from development to cancer, Nat. Rev. Cancer 10 (2010) 116–129.
[10] S.N. Stacey, A. Manolescu, P. Sulem, et al., Common variants on chromosome 5p12 confer susceptibility to estrogen receptor-positive breast cancer, Nat. Genet. 40 (2008) 703–706.
[11] A. Dutt, H.B. Salvesen, T.H. Chen, et al., Drug-sensitive FGFR2 mutations in endometrial carcinoma, Proc. Natl. Acad. Sci. USA 105 (2008) 8713–8717.
[12] D.M. Ornitz, P.J. Marie, FGF signaling pathways in endochondral and intramembranous bone development and human genetic disease, Genes Dev. 16 (2002) 1446–1465.
[13] K. Kunii, D.J. Gorenstein, H. Hatch, et al., FGFR2-amplified gastric cancer cell lines require FGFR2 and Erbb3 signaling for growth and survival, Cancer Res. 68 (2008) 2340–2348.
[14] E.A. Mittendorf, Y. Wu, M. Scaltriti, et al., Loss of HER2 amplification following trastuzumab-based neoadjuvant systemic therapy and survival outcomes, Clin. Cancer Res. 15 (2009) 7381–7388.

British Journal of Cancer (2011), 1–8

www.bjcancer.com

Full Paper

Thymidylate synthase as a determinant of pemetrexed sensitivity in non-small cell lung cancer

K Takezawa[1], I Okamoto*[,1], W Okamoto[1], M Takeda[1], K Sakai[2], S Tsukioka[3], K Kuwata[1], H Yamaguchi[1], K Nishio[2] and K Nakagawa[1]

[1]Department of Medical Oncology, Kinki University Faculty of Medicine, 377-2 Ohno-higashi, Osaka-Sayama, Osaka 589-8511, Japan; [2]Department of Genome Biology, Kinki University Faculty of Medicine, 377-2 Ohno-higashi, Osaka-Sayama, Osaka 589-8511, Japan; [3]Tokushima Research Center, Taiho Pharmaceutical Co. Ltd., 224-2 Hiraishi-ebisuno, Kawauchi, Tokushima 771-0194, Japan

BACKGROUND: Although a high level of thymidylate synthase (TS) expression in malignant tumours has been suggested to be related to a reduced sensitivity to the antifolate drug pemetrexed, no direct evidence for such an association has been demonstrated in non-small cell lung cancer (NSCLC). We have now investigated the effect of TS overexpression on pemetrexed sensitivity in NSCLC cells.
METHODS: We established NSCLC cell lines that stably overexpress TS and examined the effects of such overexpression on the cytotoxicity of pemetrexed both *in vitro* and in xenograft models. We further examined the relation between TS expression in tumour specimens from NSCLC patients and the tumour response to pemetrexed by immunohistochemical analysis.
RESULTS: The sensitivity of NSCLC cells overexpressing TS to the antiproliferative effect of pemetrexed was markedly reduced compared with that of control cells. The inhibition of DNA synthesis and induction of apoptosis by pemetrexed were also greatly attenuated by forced expression of TS. Furthermore, tumours formed by TS-overexpressing NSCLC cells in nude mice were resistant to the growth-inhibitory effect of pemetrexed observed with control tumours. Finally, the level of TS expression in tumours of non-responding patients was significantly higher than that in those of responders, suggestive of an inverse correlation between TS expression and tumour response to pemetrexed.
CONCLUSION: A high level of TS expression confers a reduced sensitivity to pemetrexed. TS expression is thus a potential predictive marker for response to pemetrexed-based chemotherapy in NSCLC patients.
British Journal of Cancer advance online publication, 12 April 2011; doi:10.1038/bjc.2011.129 www.bjcancer.com

Keywords: non-small cell lung cancer; thymidylate synthase; pemetrexed; apoptosis; immunohistochemistry

Lung cancer is the most common cause of cancer-related death worldwide, with non-small cell lung cancer (NSCLC) accounting for ~75% of all lung cancer cases (Hoffman *et al*, 2000). Platinum-based chemotherapy is the standard first-line treatment for individuals with advanced NSCLC, but the efficacy of such agents with regard to improving clinical outcome is limited (Schiller *et al*, 2002). Both experimental and clinical studies have revealed that many molecules contribute to the biological activities of malignant tumours including NSCLC. New strategies based on a better understanding of tumour biology may thus help to maximise the efficacy of current treatments.

A relatively new antifolate drug, pemetrexed, inhibits the growth of a variety of tumour types by targeting multiple folate-dependent enzymes including thymidylate synthase (TS), dihydrofolate reductase, and glycinamide ribonucleotide formyltransferase (Shih *et al*, 1997). The antitumour efficacy of pemetrexed has been found to be more limited in lung cancer patients with squamous cell carcinoma than in those with other histotypes of NSCLC (Scagliotti *et al*, 2008). Furthermore, the abundance of TS mRNA or protein seems to be higher in squamous cell carcinoma than in other histotypes of NSCLC (Ceppi *et al*, 2006; Monica *et al*, 2009; Takezawa *et al*, 2010), and high levels of TS expression in various tumour types have been suggested to correlate with a poor response to TS-targeted agents (Johnston *et al*, 1994, 1997; Pestalozzi *et al*, 1997; Ferguson *et al*, 1999). The poorer response of NSCLC patients with squamous cell carcinoma to pemetrexed is thus thought to result from the higher level of TS expression in such tumours. However, such a relation between a high TS expression level and a reduced sensitivity to pemetrexed in NSCLC has not been well established. Moreover, the precise mechanism that might underlie a reduced sensitivity to pemetrexed in tumours with a high level of TS expression remains unknown.

We have now constructed an expression vector for TS and have used this vector to establish several NSCLC cell lines that stably overexpress TS. With the use of these cells, we examined the relation between the anticancer effects of pemetrexed both *in vitro* and *in vivo* and the expression level of TS. We further investigated the relation between pemetrexed sensitivity and TS expression level in primary lung cancer patients.

MATERIALS AND METHODS

Cell culture and reagents

The human lung cancer cell lines A549, H1299, and PC9 were obtained from American Type Culture Collection (Manassas, VA, USA).

*Correspondence: Dr I Okamoto;
E-mail: chi-okamoto@dotd.med.kindai.ac.jp
Revised 9 March 2011; accepted 21 March 2011

All cells were cultured in RPMI 1640 medium (Sigma, St Louis, MO, USA) supplemented with 10% fetal bovine serum and 1% penicillin-streptomycin (Sigma), and they were maintained under a humidified atmosphere of 5% CO_2 at 37°C. Pemetrexed, cisplatin, and docetaxel were obtained from Wako (Osaka, Japan).

Generation of TS-overexpressing NSCLC cell lines

A full-length cDNA fragment encoding TS was obtained from PC9 cells by reverse transcription and the polymerase chain reaction with the primers TS-F (5′-AAGCTTCGCGCCATGCCTGTGG CCGGCTCGGAG-3′) and TS-R (5′-GCGGCCGCCTAAACAGCC ATTTCCATTTTAATAG-3′). The amplification product was verified by sequencing after its cloning into the pCR-Blunt II-TOPO vector (Invitrogen, Carlsbad, CA, USA). The TS cDNA was excised from pCR-Blunt II-TOPO and transferred to the pMZs retroviral vector (Cell Biolabs, San Diego, CA, USA). The resulting pMZs construct and the pVSV-G vector (Clontech, Palo Alto, CA, USA) for construction of the viral envelope were introduced into GP2-293 cells (~80% confluence in a 10-cm dish) with the use of the FuGENE6 transfection reagent. After 48 h, the viral particles released into the culture medium were concentrated by centrifugation at 15 000 × **g** for 3 h at 4°C. The resulting pellet was then suspended in fresh RPMI 1640 medium and used to infect A549, H1299, or PC9 cells as previously described (Okamoto *et al*, 2010).

Immunoblot analysis

Cells were washed twice with ice-cold phosphate-buffered saline (PBS) and then lysed in a solution containing 20 mM Tris-HCl (pH 7.5), 150 mM NaCl, 1 mM EDTA, 1% Triton X-100, 2.5 mM sodium pyrophosphate, 1 mM phenylmethylsulfonyl fluoride, and leupeptin (1 $\mu g\,ml^{-1}$). The protein concentration of cell lysates was determined with the Bradford reagent (Bio-Rad, Hercules, CA, USA), and equal amounts of lysate protein were subjected to SDS-polyacrylamide gel electrophoresis on a 7.5 or 12% gel. The separated proteins were transferred to a nitrocellulose membrane, which was then exposed to 5% non-fat dried milk in PBS for 1 h at room temperature before incubation overnight at 4°C with primary antibodies. Rabbit polyclonal antibodies to human TS were obtained from Santa Cruz Biotechnology (Santa Cruz, CA, USA), and those to β-actin were from Sigma. The membrane was then washed with PBS containing 0.05% Tween 20 before incubation for 1 h at room temperature with horseradish peroxidase-conjugated goat antibodies to rabbit immunoglobulin G (Sigma). Immune complexes were finally detected with chemiluminescence reagents (GE Healthcare, Little Chalfont, UK).

Assay of TS activity

Thymidylate synthase activity was quantified with the use of a tritiated 5-fluoro-dUMP binding assay. Cells were harvested, diluted in 0.2 M Tris-HCl (pH 7.4) containing 20 mM 2-mercaptoethanol, 15 mM CMP, and 100 mM NaF, and disrupted by ultrasonic treatment. The cell lysate was centrifuged at 1600 × **g** for 15 min at 4°C, and the resulting supernatant was centrifuged at 105 000 × **g** for 1 h at 4°C. A portion (50 μl) of the final supernatant was mixed consecutively with 50 μl of Buffer A (600 mM NH_4HCO_3 buffer (pH 8.0), 100 mM 2-mercaptoethanol, 100 mM NaF, 15 mM CMP) and with 50 μl of (6-^{3}H)5-fluoro-dUMP (7.8 pmol) plus 25 μl of cofactor solution (50 mM potassium phosphate buffer (pH 7.4), 20 mM 2-mercaptoethanol, 100 mM NaF, 15 mM CMP, 2% bovine serum albumin, 2 mM tetrahydrofolic acid, 16 mM sodium ascorbate, 9 mM formaldehyde). The resulting mixture was incubated at 30°C for 20 min, after which the reaction was terminated by the addition of 100 μl of 2% bovine serum albumin and 275 μl of 1 M $HClO_4$ and by centrifugation at 1600 × **g** for 15 min at 4°C. The resulting precipitate was suspended in 2 ml of 0.5 M $HClO_4$, and the mixture was subjected to ultrasonic treatment followed by centrifugation at 1600 × **g** for 15 min at 4°C. The final precipitate was solubilised with 0.5 ml of 98% formic acid, mixed with 10 ml of ACS II scintillation fluid, and assayed for radioactivity. Data are expressed as picomoles of substrate consumed per milligram of soluble protein.

Cell growth inhibition assay *in vitro* (MTT assay)

Cells were plated in 96-well flat-bottomed plates and cultured for 24 h before exposure to various concentrations of drugs for 72 h. TetraColor One (5 mM tetrazolium monosodium salt and 0.2 mM 1-methoxy-5-methyl phenazinium methylsulfate; Seikagaku, Tokyo, Japan) was then added to each well, and the cells were incubated for 3 h at 37°C before measurement of absorbance at 490 nm with a Multiskan Spectrum instrument (Thermo Labsystems, Boston, MA, USA).

RNA interference

Cells were plated at 50–60% confluence in six-well plates or 25-cm^2 flasks and then incubated for 24 h before transient transfection for the indicated times with small interfering RNAs (siRNAs) mixed with the Lipofectamine reagent (Invitrogen). An siRNA specific for human TS mRNA (5′-CAAUCCGCAUCCAA CUAUU-3′) and a nonspecific siRNA (5′-GUUGAGAGAUAUUA GAGUU-3′) was obtained from Nippon EGT (Toyama, Japan).

Assay of DNA synthesis

DNA synthesis was measured with the use of a Cell Proliferation ELISA BrdU Kit (Roche, Basel, Switzerland). In brief, cells were seeded in 96-well plates at a density of 10 000–20 000 per well and exposed to various concentrations of drugs for 48 h. They were then incubated in the additional presence of bromodeoxyuridine (BrdU) for 3 h before exposure to detection reagents for 15 min at 25°C and measurement of luminescence.

Annexin V binding assay

Binding of annexin V to cells was measured with the use of an Annexin-V-FLUOS Staining Kit (Roche). Cells were harvested by exposure to trypsin–EDTA, washed with PBS, and centrifuged at 200 × **g** for 5 min. The cell pellets were resuspended in 100 μl of Annexin-V-FLUOS labelling solution, incubated for 10–15 min at 15 to 25°C, and then analysed for fluorescence with a flow cytometer (FACS Calibur) (Becton Dickinson, San Jose, CA, USA) and Cell Quest software (Becton Dickinson).

Animals

Male athymic nude mice were maintained on a 12-h light, 12-h dark cycle and provided with food and water ad libitum in a barrier facility. All animal experiments were carried out with approval of the institutional animal care and use committee and complied with the specifications of the Association for Assessment and Accreditation of Laboratory Animal Care of Japan.

Tumour growth inhibition assay *in vivo*

Cubic fragments of tumour tissue (~2 by 2 by 2 mm) were implanted subcutaneously into the axilla of 5- to 6-week-old male athymic nude mice. Treatment was initiated when tumours in each group of eight mice achieved an average volume of 150–200 mm^3. Pemetrexed (100 mg per kilogram of body weight) or vehicle (physiological saline) was administered intraperitoneally once a week. Tumour volume was determined from caliper measurements of tumour length (L) and width (W) according to the formula $LW^2/2$. Both tumour size and body weight were measured twice per week.

Patients and clinical specimens

For retrospective analysis, we recruited consecutive patients with advanced NSCLC who received chemotherapy at Kinki University Hospital between April 2008 and June 2010. Patients met all of the following criteria: a histological diagnosis of NSCLC with at least one measurable lesion; a clinical stage of 3B or 4; an Eastern Cooperative Oncology Group (ECOG) performance status of 0 or 1; adequate haematologic, hepatic, and renal function; treatment either with carboplatin at an area under the curve (AUC) of 5 on day 1 and pemetrexed at 500 mg m^{-2} on day 1 of an 21-day cycle or with cisplatin at 75 mg m^{-2} on day 1 and pemetrexed at 500 mg m^{-2} on day 1 of an 21-day cycle as first-line chemotherapy; and availability of sufficient tumour tissue in paraffin blocks for assessment by immunohistochemistry. Tumour tissue specimens were obtained by transbronchial lung biopsy. Tumour response was examined by computed tomography and evaluated according to the Response Evaluation Criteria in Solid tumours (RECIST) as complete response (CR), partial response (PR), stable disease (SD), or progressive disease (PD). This study conforms to the provisions of the Declaration of Helsinki and was approved by the local institutional review board.

Immunohistochemistry and scoring of TS expression

Paraffin-embedded sections (thickness, 4 μm) of tumour tissue were depleted of paraffin with xylene and then rehydrated, and endogenous peroxidase activity was quenched by incubation with 0.3% hydrogen peroxide in methanol. Antigen retrieval was carried out by microwave irradiation for 10 min in citrate buffer (pH 6.0). The sections were then washed with PBS before incubation overnight at room temperature with rabbit polyclonal antibodies to TS (Taiho Pharmaceutical Co., Saitama, Japan) at a dilution of 1 : 100. Immune complexes were detected by incubation at room temperature for 30 min first with biotinylated goat antibodies to rabbit immunoglobulin G (Dako, Santa Barbara, CA, USA) and then with streptavidin-conjugated horseradish peroxidase (Dako).

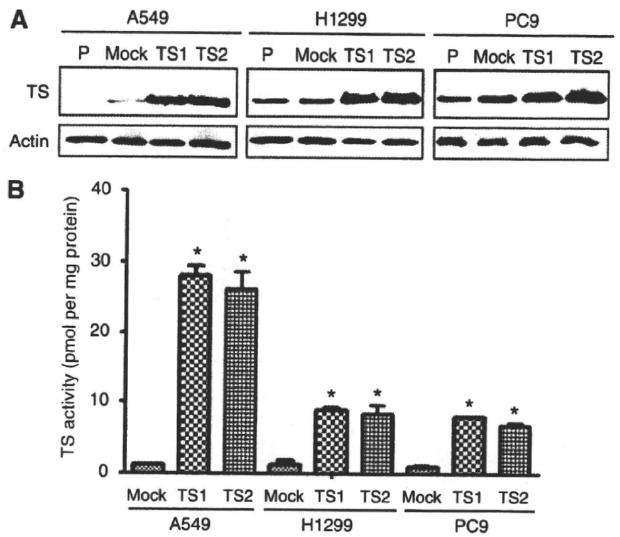

Figure 1 Abundance and enzymatic activity of TS in TS-overexpressing NSCLC cell lines. Parental (P) A549, H1299, or PC9 cells or corresponding sublines either stably overexpressing TS (TS1 and TS2) or harbouring the empty vector (Mock) were cultured overnight in complete medium, after which cell lysates were prepared and either subjected to immunoblot analysis with antibodies to TS and to β-actin (loading control) (**A**) or assayed for TS activity. (**B**) Data are means ± s.d. of triplicates from experiments that were repeated on two additional occasions with similar results. *$P<0.05$ *vs* the corresponding value for Mock cells (Student's two-tailed *t*-test).

Peroxidase activity was visualised with diaminobenzidine tetrahydrochloride solution (Dako), and the sections were counterstained with hematoxylin before examination with a microscope (Dako). The human colon cancer cell line DLD-1/FrUrd, human breast cancer cell line MDA-MB-435S, and human pancreatic cancer cell line MIAPaCa-2 (all obtained from American Type Culture Collection) were used as positive controls for TS staining. All immunostained sections were reviewed by two observers without knowledge of the patients' characteristics. Sections with discrepant results were jointly reevaluated until a consensus was reached. Cytoplasmic staining for TS was scored in a semiquantitative manner, reflecting both the intensity of staining and the percentage of cells with staining at each intensity. Staining intensity was classified as 0 (no staining), +1 (weak staining), +2 (distinct staining), or +3 (strong staining). A value designated the HSCORE was obtained as $\Sigma(I \times PC)$, where I and

Table 1 Median inhibitory concentrations (μM) for the antiproliferative effects of chemotherapeutic agents in TS-overexpressing NSCLC cells *in vitro*

Cell line	Pemetrexed	Cisplatin	Docetaxel
A549/Mock	0.07	2.62	0.12
A549/TS1	0.38	2.37	0.12
A549/TS2	0.44	2.21	0.13
H1299/Mock	0.08	2.93	0.32
H1299/TS1	0.22	2.98	0.30
H1299/TS2	0.22	2.90	0.30
PC9/Mock	0.03	0.72	0.18
PC9/TS1	0.11	0.72	0.18
PC9/TS2	0.10	0.65	0.17

Abbreviations: NSCLC = non-small cell lung cancer; TS = thymidylate synthase.

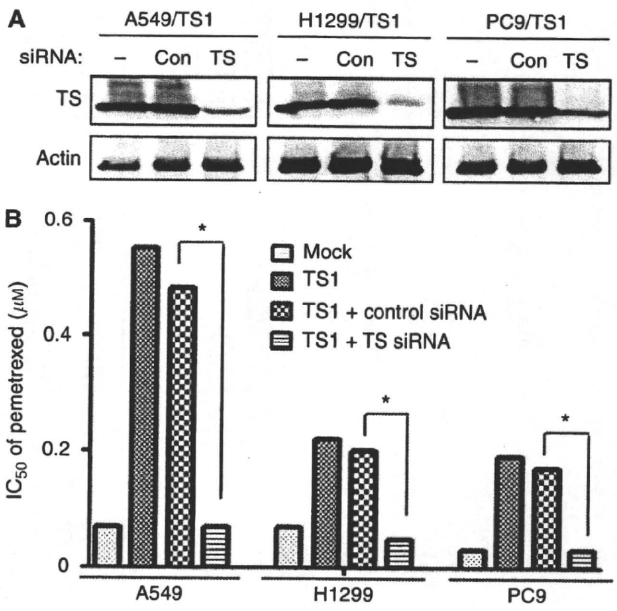

Figure 2 Effect of TS depletion on pemetrexed sensitivity in TS-overexpressing NSCLC cells. (**A**) Cells of the indicated lines were transfected or not (–) with nonspecific (Con) or TS siRNAs for 48 h, after which cell lysates were subjected to immunoblot analysis with antibodies to TS and to β-actin. (**B**) Cells transfected as in **A** were cultured for 72 h in complete medium containing various concentrations of pemetrexed, after which cell viability was assessed as described in Materials and methods section, and the median inhibitory concentration (IC_{50}) of pemetrexed was determined. Data are means of triplicates from experiments that were repeated on two additional occasions with similar results. *$P<0.05$ (Student's two-tailed *t*-test).

PC represent staining intensity and the percentage of cells that stain at each intensity, respectively. The selection of a clinically important cutoff score for TS expression was based on receiver operating characteristic (ROC) curve analysis.

Statistical analysis

Quantitative data are presented as means ± s.d. or ± s.e.m. as indicated, and were analysed by Student's two-tailed *t*-test. Progression-free survival was assessed from the first day of chemotherapy administration to the date of objective disease progression. Kaplan–Meier analysis was used to estimate the probability of survival as a function of time, and differences in the survival of subgroups of patients were evaluated with the log-rank test. A *P*-value of <0.05 was considered statistically significant.

RESULTS

Forced expression of TS reduces the sensitivity of NSCLC cells to pemetrexed

To investigate whether the level of TS expression affects the sensitivity of NSCLC cells to pemetrexed, we first established A549 (A549/TS1 and A549/TS2), H1299 (H1299/TS1 and H1299/TS2), and PC9 (PC9/TS1 and PC9/TS2) cells that stably overexpress TS. Cells that stably harbour the corresponding empty vector (A549/Mock, H1299/Mock, and PC9/Mock) were established as controls. Immunoblot analysis showed that the abundance of TS was markedly increased in the TS-overexpressing lines compared with the parental or Mock cells (Figure 1A). The enzymatic activity of TS was also substantially higher in the TS-overexpressing cells than in the parental or Mock cells (Figure 1B). We then examined the effect of forced expression of TS on the cytotoxicity of anticancer drugs as determined with the MTT assay. The median inhibitory concentration of pemetrexed for the TS-overexpressing cells was about three to six times that for the corresponding Mock cells for all three lung cancer lines, whereas cisplatin and docetaxel inhibited the growth of the TS-overexpressing cells in a manner similar to that observed with the corresponding Mock cells (Table 1). To exclude the possibility that these results were because of nonspecific effects of transfection, we depleted A549/TS1, H1299/TS1, and PC9/TS1 cells of TS by RNA interference. Immunoblot analysis revealed that transfection of these cells with an siRNA specific for TS mRNA resulted in downregulation of the corresponding protein (Figure 2A). This reduction in the abundance of TS restored the sensitivity of the cells to the

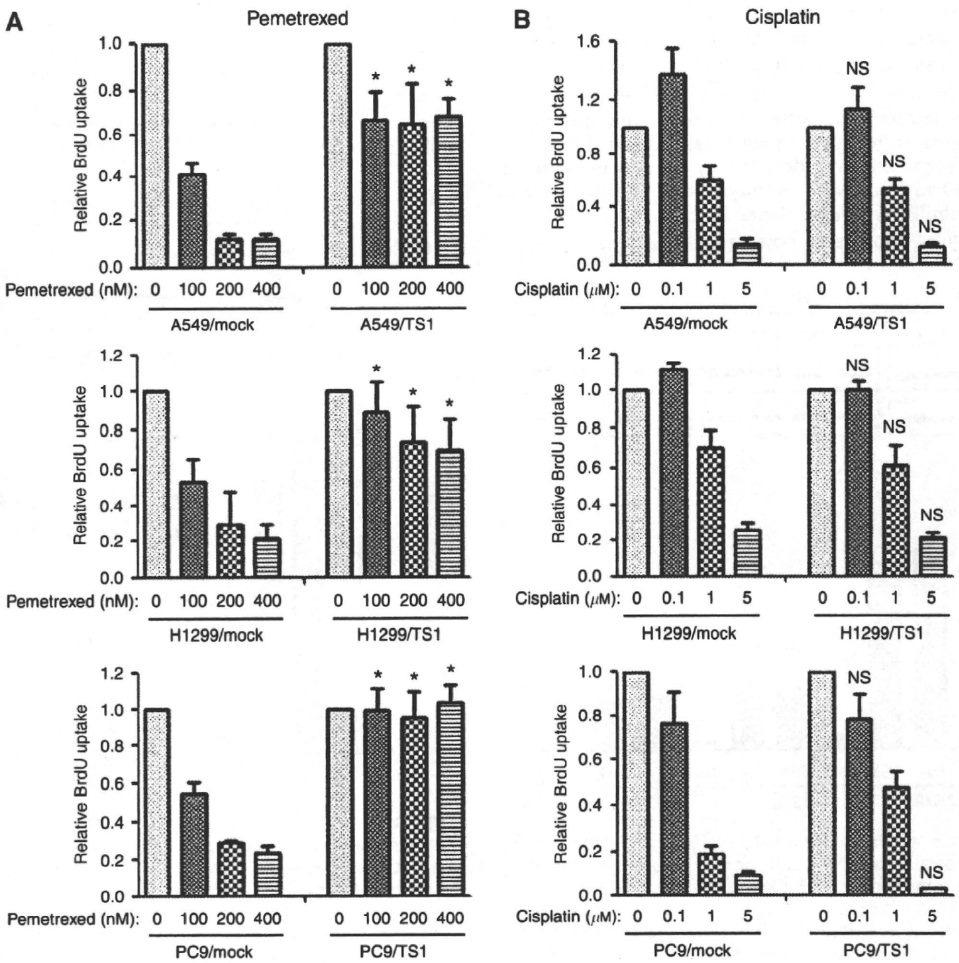

Figure 3 Effects of pemetrexed and cisplatin on DNA synthesis in NSCLC cells overexpressing TS. The indicated NSCLC cell lines were cultured for 48 h in complete medium containing various concentrations of pemetrexed (**A**) or cisplatin (**B**), after which BrdU incorporation was assessed as described in Materials and methods section. Data are means ± s.d. of triplicates from experiments that were repeated a total of three times with similar results. $^*P<0.05$ *vs* the corresponding value for Mock cells (Student's two-tailed *t*-test). NS, not significant.

inhibitory effect of pemetrexed on cell growth (Figure 2B). These data thus indicated that high TS expression levels reduce the sensitivity of NSCLC cells to pemetrexed.

Effects of chemotherapeutic agents on DNA synthesis and apoptosis in TS-overexpressing NSCLC cell lines

We next investigated the effects of TS overexpression on DNA synthesis and apoptosis in NSCLC cells exposed to pemetrexed, given that the cytotoxic activity of pemetrexed is due to inhibition of DNA synthesis and subsequent induction of apoptosis. Assay of BrdU incorporation revealed that pemetrexed inhibited DNA synthesis in Mock cell lines in a concentration-dependent manner, whereas this effect was much less pronounced in the TS-overexpressing lines (Figure 3A). In contrast, the concentration-dependent inhibition of DNA synthesis by cisplatin was largely unaffected by forced expression of TS (Figure 3B). An annexin V binding assay also revealed that the frequency of apoptosis was markedly increased by pemetrexed in a concentration-dependent manner in Mock cells, whereas pemetrexed had little effect on apoptosis in cells overexpressing TS (Figure 4A). To confirm that this attenuation of pemetrexed-induced apoptosis in TS-overexpressing cells was due to the forced expression of TS, we depleted the TS-overexpressing cells of TS by transfection with the TS siRNA and then examined the effect of pemetrexed on apoptosis. Downregulation of TS expression restored the sensitivity of these cells to the proapoptotic effect of pemetrexed. In contrast to pemetrexed, cisplatin increased the proportion of apoptotic cells among Mock and TS-overexpressing cells to similar extents (Figure 4C). These data thus suggested that the effects of pemetrexed on DNA synthesis and apoptosis are inversely related to the level of TS expression.

Effects of pemetrexed on the growth of TS-overexpressing NSCLC cells *in vivo*

We next investigated whether TS-overexpressing NSCLC cell lines might exhibit resistance to pemetrexed treatment in xenograft models. When their tumours became palpable, athymic nude mice were divided into two groups and treated with vehicle or pemetrexed for 3–4 weeks. Although pemetrexed significantly inhibited the growth of tumours formed by Mock cells of the A549, H1299, or PC9 lines, it did not exhibit such an effect with tumours formed by the corresponding TS-overexpressing cells (Figure 5). These data thus suggested that the antitumour effect of pemetrexed is suppressed by TS overexpression in NSCLC cells, consistent with our results obtained *in vitro*.

TS expression in tumours of NSCLC patients treated with pemetrexed

To evaluate the relation between the level of TS expression in NSCLC tumours and the clinical response to pemetrexed, we performed semiquantitative immunohistochemical analysis on tumour biopsy specimens from 24 patients with advanced NSCLC treated with pemetrexed combined with platinum agents

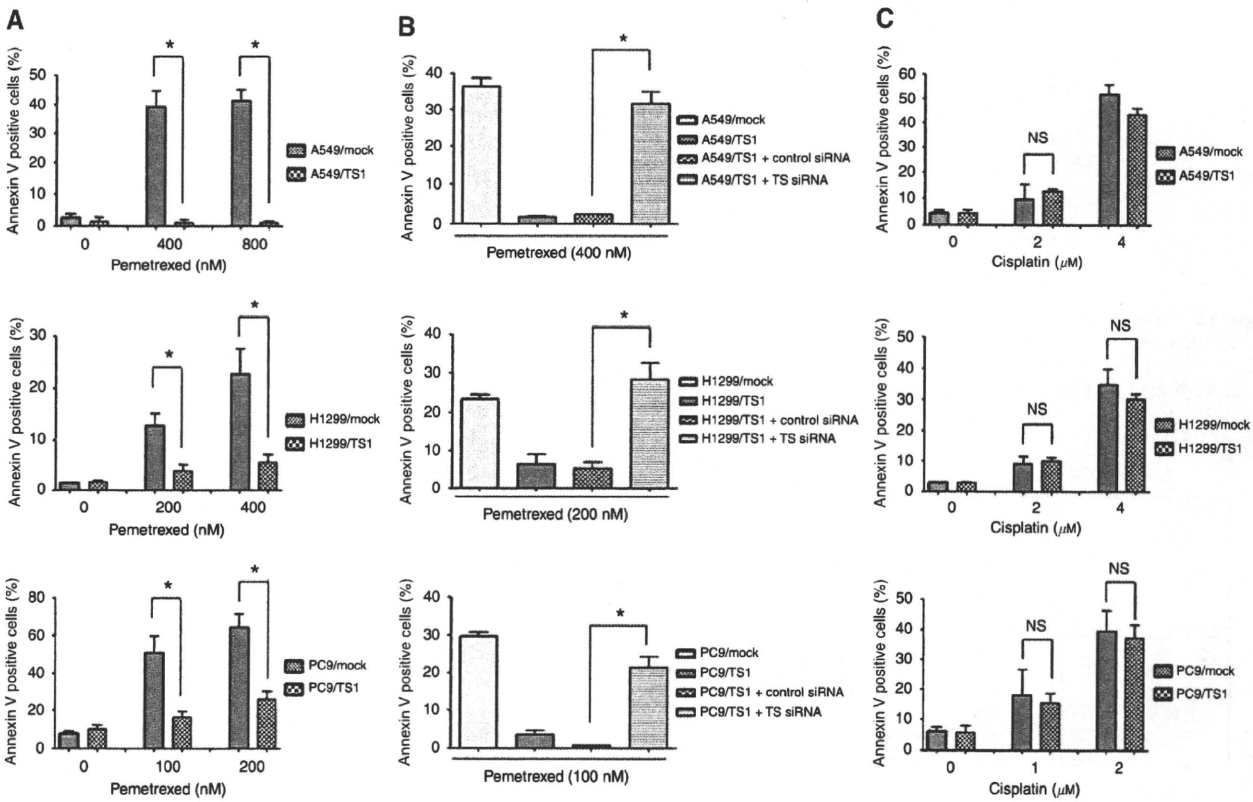

Figure 4 Effects of pemetrexed and cisplatin on apoptosis in NSCLC cells overexpressing TS. (**A** and **C**) The indicated NSCLC cell lines were cultured for 72 h in complete medium containing various concentrations of pemetrexed (**A**) or cisplatin (**C**), after which the proportion of apoptotic cells was assessed by staining with fluorescein isothiocyanate-conjugated annexin V and propidium iodide followed by flow cytometry. (**B**) The indicated NSCLC cell lines were cultured for 72 h in complete medium containing the indicated concentrations of pemetrexed with or without nonspecific (control) or TS siRNAs, after which the proportion of apoptotic cells was assessed as in **A** and **C**. All data are means ± s.d. of triplicates from experiments that were repeated a total of three times with similar results. $^*P<0.05$ (Student's two-tailed *t*-test). NS, not significant.

(Figure 6A). The characteristics of the patients are shown in Table 2. Tumours were categorised as either responding (CR or PR) or non-responding (SD or PD). The level of TS expression for non-responding groups was significantly ($P=0.038$) higher than that for responding groups (Figure 6B). We next carried out ROC curve analysis to establish the optimal cutoff value for the HSCORE of TS expression level, yielding a value of 257.5. Patients with a low level of TS expression (HSCORE$<$257.5) had a significantly longer progression-free survival ($P=0.014$) than did those with a high level (HSCORE$\geqslant$257.5) (Figure 6C). These data thus suggested that TS expression level in advanced NSCLC tumours is inversely correlated with the response to pemetrexed.

DISCUSSION

In this study, we have investigated the effects of TS overexpression on the sensitivity of NSCLC cells to pemetrexed. Pemetrexed-resistant lung cancer cell lines established by stepwise exposure to increasing concentrations of pemetrexed were recently shown to contain increased amounts of TS mRNA compared with parental cells (Ozasa *et al*, 2010). Other previous studies have also found that sensitivity to pemetrexed is inversely related to the level of TS expression in cancer cell lines (Sigmond *et al*, 2003; Giovannetti *et al*, 2008). These observations have suggested that TS gene expression is associated with resistance to pemetrexed, but the

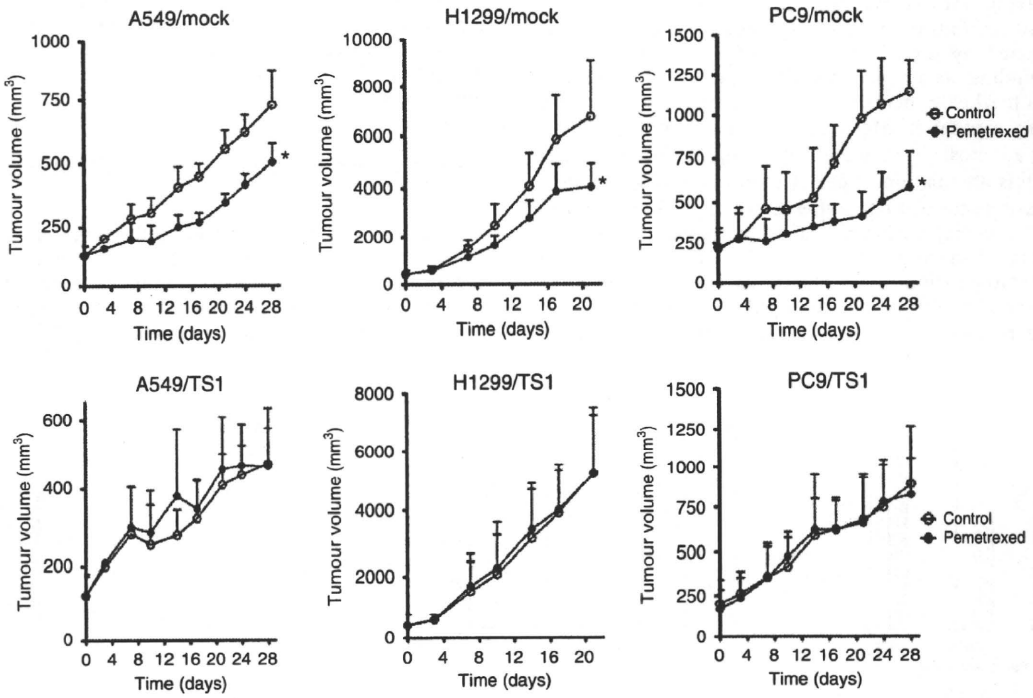

Figure 5 Effect of pemetrexed on the growth of TS-overexpressing NSCLC cells *in vivo*. Nude mice with tumour xenografts established by subcutaneous implantation of tumour fragments derived from the indicated NSCLC cell lines were treated with vehicle (control) or pemetrexed (100 mg kg^{-1}, intraperitoneal) on days 1, 8, 15, and 22. Tumour volume was determined at the indicated times after the onset of treatment. Data are means ± s.e.m. of values from eight mice per group. *$P<0.05$ for pemetrexed *vs* the corresponding value for vehicle (Student's two-tailed *t*-test).

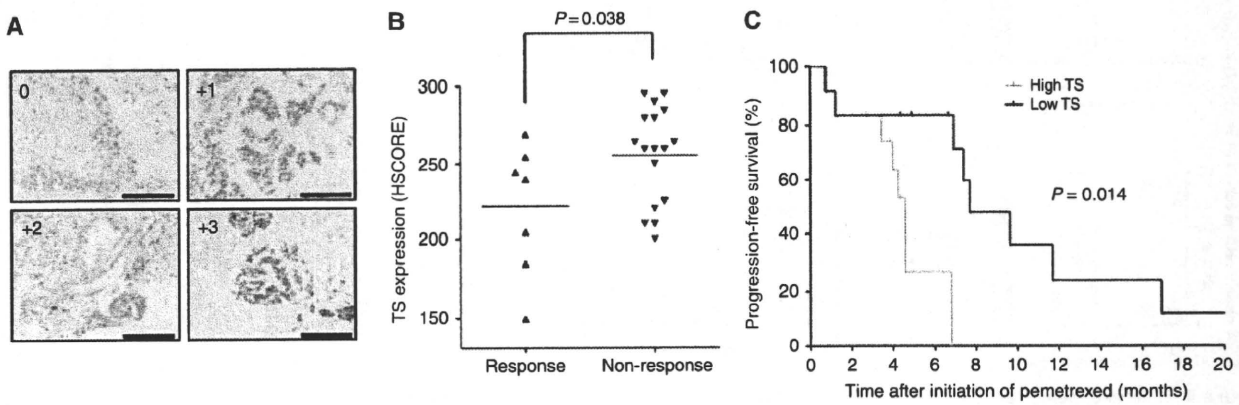

Figure 6 Relation of TS expression level to tumour response in NSCLC patients treated with pemetrexed and either carboplatin or cisplatin. (**A**) Representative sections of carcinomas including cells with the indicated intensities of TS immunostaining. Scale bars, 125 μm. (**B**) TS expression level (HSCORE) for the clinical specimens of 24 patients classified according to tumour response (response = CR or PR, $n=7$; non-response = SD or PD, $n=17$). Horizontal lines indicate mean values. The *P* value was determined by Student's two-tailed *t* test. (**C**) Progression-free survival of the NSCLC patients according to the expression level of TS in tumour specimens. The *P*-value was determined with the log-rank test.

Table 2 Patient characteristics

Characteristic	
Sex	
Male	17
Female	7
Mean (range) age (years)	66 (38–85)
Chemotherapy	
Carboplatin+pemetrexed	23
Cisplatin+pemetrexed	1
Tumor histology	
Adenocarcinoma	21
Squamous cell	1
Other	2
Disease stage	
IIIB	7
IV	17
Tumor response	
CR+PR	7
SD	13
PD	4

Abbreviations: CR = complete response; PD = progressive disease; PR = partial response; SD = stable disease.

mechanism by which a high level of TS expression might result in a reduced sensitivity to pemetrexed has remained unclear. Thymidylate synthase has a central role in the biosynthesis of thymidylate, an essential precursor for DNA synthesis (Carreras and Santi, 1995). We have previously shown that TS expression level differs among lung cancer cell lines, and that RNA interference-mediated depletion of TS in such cell lines resulted in growth suppression through inhibition of DNA synthesis and induction of apoptosis in a manner independent of the original level of TS activity (Takezawa *et al*, 2010). Pemetrexed exerts its cytotoxic effects through inhibition of multiple DNA synthesis-related enzymes including TS. We have now shown that pemetrexed inhibited DNA synthesis and induced apoptosis in NSCLC cell lines; however, it failed to induce such effects in the corresponding cells engineered to overexpress TS. Forced expression of TS also abolished the antitumour effect of pemetrexed in xenograft models. Our data suggest that pemetrexed did not fully inhibit TS activity in TS-overexpressing cells, given that DNA synthesis remained active after pemetrexed exposure. They further suggest that the observed reduction in the sensitivity of TS-overexpressing cells to pemetrexed may result from sustained activity of TS in the presence of the drug. We also examined the possible effect of pemetrexed on the expression levels of apoptosis-related molecules in both Mock and TS-overexpressing cells, but we found that pemetrexed did not substantially alter the abundance of such proteins including that of XIAP (data not shown), which we previously identified as having a key role in TS depletion-induced apoptosis in NSCLC cells (Takezawa *et al*, 2010). The precise mechanism by which pemetrexed induces apoptosis thus remains to be determined.

Previous studies have examined the possible relation between TS expression level and the response to pemetrexed in cancer patients (Gomez *et al*, 2006; Righi *et al*, 2010; Uramoto *et al*, 2010). In a phase II trial of pemetrexed monotherapy for advanced breast cancer (Gomez *et al*, 2006), 61 patients were treated with pemetrexed and evaluable for response. This study revealed a potential association between a high level of TS mRNA and a poor response to pemetrexed treatment. Another study evaluated TS expression level immunohistochemically by means of the HSCORE system in 60 patients with malignant mesothelioma treated either with the combination of pemetrexed and platinum, or with pemetrexed alone (Righi *et al*, 2010). A significant inverse correlation was found between TS expression level and time to progression, or overall survival. Finally, no significant correlation between the abundance of TS mRNA and clinical outcome was apparent for five NSCLC patients treated with the combination of pemetrexed and platinum, or with pemetrexed alone (Uramoto *et al*, 2010), although the small sample number precluded any definitive conclusion. In this study, we found that a high level of TS expression in human NSCLC tumours was significantly associated with a reduced tumour response and a shorter progression-free survival in 24 patients treated with pemetrexed combined with platinum agents, consistent with the previous studies of patients with breast cancer or malignant mesothelioma (Gomez *et al*, 2006; Righi *et al*, 2010). Given that the anticancer effects of cisplatin were independent of TS expression level in NSCLC cell lines, the relation between TS expression level and clinical outcome observed in our clinical analysis likely reflects the effect of pemetrexed. We recently evaluated the abundance of TS in NSCLC tumours of patients treated with carboplatin and paclitaxel, and neither a prognostic nor predictive role was identified for TS expression level in these patients (Takeda *et al*, 2010). Together with such observations, our present results suggest that assessment of baseline TS expression may be of predictive value in evaluation of chemosensitivity to pemetrexed in NSCLC. Although we cannot exclude a contribution of factors other than TS expression level to pemetrexed chemosensitivity, our preclinical and clinical data provide a rationale for the potential use of TS expression level as a predictive biomarker for response to pemetrexed or pemetrexed-based chemotherapy in patients with NSCLC. Further investigation is needed with a larger cohort of patients or in prospective studies to confirm this conclusion.

REFERENCES

Carreras CW, Santi DV (1995) The catalytic mechanism and structure of thymidylate synthase. *Annu Rev Biochem* **64:** 721–762

Ceppi P, Volante M, Saviozzi S, Rapa I, Novello S, Cambieri A, Lo Iacono M, Cappia S, Papotti M, Scagliotti GV (2006) Squamous cell carcinoma of the lung compared with other histotypes shows higher messenger RNA and protein levels for thymidylate synthase. *Cancer* **107:** 1589–1596

Ferguson PJ, Collins O, Dean NM, DeMoor J, Li CS, Vincent MD, Koropatnick J (1999) Antisense down-regulation of thymidylate synthase to suppress growth and enhance cytotoxicity of 5-FUdR, 5-FU and Tomudex in HeLa cells. *Br J Pharmacol* **127:** 1777–1786

Giovannetti E, Lemos C, Tekle C, Smid K, Nannizzi S, Rodriguez JA, Ricciardi S, Danesi R, Giaccone G, Peters GJ (2008) Molecular mechanisms underlying the synergistic interaction of erlotinib, an epidermal growth factor receptor tyrosine kinase inhibitor, with the multitargeted antifolate pemetrexed in non-small-cell lung cancer cells. *Mol Pharmacol* **73:** 1290–1300

Gomez HL, Santillana SL, Vallejos CS, Velarde R, Sanchez J, Wang X, Bauer NL, Hockett RD, Chen VJ, Niyikiza C, Hanauske AR (2006) A phase II trial of pemetrexed in advanced breast cancer: clinical response and association with molecular target expression. *Clin Cancer Res* **12:** 832–838

Hoffman PC, Mauer AM, Vokes EE (2000) Lung cancer. *Lancet* **355:** 479–485

Johnston PG, Fisher ER, Rockette HE, Fisher B, Wolmark N, Drake JC, Chabner BA, Allegra CJ (1994) The role of thymidylate synthase expression in prognosis and outcome of adjuvant chemotherapy in patients with rectal cancer. *J Clin Oncol* **12:** 2640–2647

Johnston PG, Mick R, Recant W, Behan KA, Dolan ME, Ratain MJ, Beckmann E, Weichselbaum RR, Allegra CJ, Vokes EE (1997) Thymidylate synthase expression and response to neoadjuvant

chemotherapy in patients with advanced head and neck cancer. *J Natl Cancer Inst* **89:** 308–313

Monica V, Scagliotti GV, Ceppi P, Righi L, Cambieri A, Lo Iacono M, Saviozzi S, Volante M, Novello S, Papotti M (2009) Differential thymidylate synthase expression in different variants of large-cell carcinoma of the lung. *Clin Cancer Res* **15:** 7547–7552

Okamoto W, Okamoto I, Tanaka K, Hatashita E, Yamada Y, Kuwata K, Yamaguchi H, Arao T, Nishio K, Fukuoka M, Janne PA, Nakagawa K (2010) TAK-701, a humanized monoclonal antibody to hepatocyte growth factor, reverses gefitinib resistance induced by tumor-derived HGF in non-small cell lung cancer with an EGFR mutation. *Mol Cancer Ther* **9:** 2785–2792

Ozasa H, Oguri T, Uemura T, Miyazaki M, Maeno K, Sato S, Ueda R (2010) Significance of thymidylate synthase for resistance to pemetrexed in lung cancer. *Cancer Sci* **101:** 161–166

Pestalozzi BC, Peterson HF, Gelber RD, Goldhirsch A, Gusterson BA, Trihia H, Lindtner J, Cortes-Funes H, Simmoncini E, Byrne MJ, Golouh R, Rudenstam CM, Castiglione-Gertsch M, Allegra CJ, Johnston PG (1997) Prognostic importance of thymidylate synthase expression in early breast cancer. *J Clin Oncol* **15:** 1923–1931

Righi L, Papotti MG, Ceppi P, Bille A, Bacillo E, Molinaro L, Ruffini E, Scagliotti GV, Selvaggi G (2010) Thymidylate synthase but not excision repair cross-complementation group 1 tumor expression predicts outcome in patients with malignant pleural mesothelioma treated with pemetrexed-based chemotherapy. *J Clin Oncol* **28:** 1534–1539

Scagliotti GV, Parikh P, von Pawel J, Biesma B, Vansteenkiste J, Manegold C, Serwatowski P, Gatzemeier U, Digumarti R, Zukin M, Lee JS, Mellemgaard A, Park K, Patil S, Rolski J, Goksel T, de Marinis F, Simms L, Sugarman KP, Gandara D (2008) Phase III study comparing cisplatin plus gemcitabine with cisplatin plus pemetrexed in chemotherapy-naive patients with advanced-stage non-small-cell lung cancer. *J Clin Oncol* **26:** 3543–3551

Schiller JH, Harrington D, Belani CP, Langer C, Sandler A, Krook J, Zhu J, Johnson DH (2002) Comparison of four chemotherapy regimens for advanced non-small-cell lung cancer. *N Engl J Med* **346:** 92–98

Shih C, Chen VJ, Gossett LS, Gates SB, MacKellar WC, Habeck LL, Shackelford KA, Mendelsohn LG, Soose DJ, Patel VF, Andis SL, Bewley JR, Rayl EA, Moroson BA, Beardsley GP, Kohler W, Ratnam M, Schultz RM (1997) LY231514, a pyrrolo[2,3-d]pyrimidine-based antifolate that inhibits multiple folate-requiring enzymes. *Cancer Res* **57:** 1116–1123

Sigmond J, Backus HH, Wouters D, Temmink OH, Jansen G, Peters GJ (2003) Induction of resistance to the multitargeted antifolate Pemetrexed (ALIMTA) in WiDr human colon cancer cells is associated with thymidylate synthase overexpression. *Biochem Pharmacol* **66:** 431–438

Takeda M, Okamoto I, Hirabayashi N, Kitano M, Nakagawa K (2010) Thymidylate synthase and dihydropyrimidine dehydrogenase expression levels are associated with response to S-1 plus carboplatin in advanced non-small cell lung cancer. *Lung Cancer*; doi:10.1016/j.lungcan.2010.10.022

Takezawa K, Okamoto I, Tsukioka S, Uchida J, Kiniwa M, Fukuoka M, Nakagawa K (2010) Identification of thymidylate synthase as a potential therapeutic target for lung cancer. *Br J Cancer* **103:** 354–361

Uramoto H, Onitsuka T, Shimokawa H, Hanagiri T (2010) TS, DHFR and GARFT expression in non-squamous cell carcinoma of NSCLC and malignant pleural mesothelioma patients treated with pemetrexed. *Anticancer Res* **30:** 4309–4315

Published OnlineFirst March 17, 2011; DOI:10.1158/1078-0432.CCR-10-2798

Clinical Cancer Research

Human Cancer Biology

Role of ERK-BIM and STAT3-Survivin Signaling Pathways in ALK Inhibitor–Induced Apoptosis in EML4-ALK–Positive Lung Cancer

Ken Takezawa[1], Isamu Okamoto[1], Kazuto Nishio[2], Pasi A. Jänne[3], and Kazuhiko Nakagawa[1]

Abstract

Purpose: *EML4-ALK* (echinoderm microtubule-associated protein–like 4 anaplastic lymphoma kinase) was recently identified as a transforming fusion gene in non–small cell lung cancer. The purpose of the present study was to characterize the mechanism of malignant transformation by EML4-ALK.

Experimental Design: We established NIH 3T3 cells that stably express variant 1 or 3 of EML4-ALK and examined the signaling molecules that function downstream of EML4-ALK.

Results: Forced expression of EML4-ALK induced marked activation of extracellular signal–regulated kinase (ERK) and STAT3, but not that of AKT. Inhibition of ERK or STAT3 signaling resulted in substantial attenuation of the proliferation of cells expressing either variant of EML4-ALK, suggesting that these signaling pathways function downstream of EML4-ALK in lung cancer cells. The specific ALK inhibitor TAE684 induced apoptosis that was accompanied both by upregulation of BIM, a proapoptotic member of the Bcl-2 family, and by downregulation of survivin, a member of the inhibitor of apoptosis protein (IAP) family, in EML4-ALK–expressing NIH 3T3 cells as well as in H3122 human lung cancer cells harboring endogenous EML4-ALK. Depletion of BIM and overexpression of survivin each inhibited TAE684-induced apoptosis, suggesting that both upregulation of BIM and downregulation of survivin contribute to TAE684-induced apoptosis in EML4-ALK–positive lung cancer cells. Furthermore, BIM and survivin expression was found to be independently regulated by ERK and STAT3 signaling pathways, respectively.

Conclusions: ALK inhibitor–induced apoptosis is mediated both by BIM upregulation resulting from inhibition of ERK signaling as well as by survivin downregulation resulting from inhibition of STAT3 signaling in EML4-ALK–positive lung cancer cells. *Clin Cancer Res; 17(8); 2140–8. ©2011 AACR.*

Introduction

Lung cancer is the leading cause of cancer deaths worldwide. Given that the efficacy of conventional chemotherapeutic agents with regard to improving clinical outcome in lung cancer patients is limited, target-based therapies are being pursued as potential treatment alternatives. Somatic mutations in the tyrosine kinase domain of the epidermal growth factor receptor (EGFR) have been associated with tumor responsiveness to EGFR tyrosine kinase inhibitors (TKI) in a subset of individuals with non–small cell lung cancer (NSCLC; refs. 1–3). Such findings suggest that the use of molecularly targeted therapy in genetically defined subsets of cancer patients may prove to be an effective strategy for the treatment of many cancers including NSCLC. Given that lung cancer is a common type of cancer, the identification of even small subsets of lung cancer patients harboring specific genetic abnormalities will translate into the provision of large cohorts for targeted therapy.

A recent study identified a potential driver mutation in NSCLC: fusion of the echinoderm microtubule-associated protein–like 4 gene (*EML4*) with the anaplastic lymphoma kinase gene (*ALK*), which results in the production of a fusion protein (EML4-ALK) consisting of the NH_2-terminal portion of EML4 and the COOH-terminal region of ALK (4). ALK was originally discovered as the result of characterization of chromosomal translocations that lead to the expression of fusion proteins consisting of the COOH-terminal kinase domain of ALK and the NH_2-terminal portion of nucleophosmin (NPM) in patients with anaplastic large cell lymphoma (5, 6). Various break and fusion points within the *EML4* locus in NSCLC cells give rise to different isoforms of EML4-ALK, which appear to be present in 5% to 10% of NSCLC cases (4, 7–14). The most common EML4-ALK variants are 1 and 3, which together account for about 60% of EML4-ALK–positive lung cancer cases (14). All EML4-ALK isoforms undergo constitutive oligomerization mediated by the coiled coil domain of the

Authors' Affiliations: Departments of [1]Medical Oncology and [2]Genome Biology, Kinki University Faculty of Medicine, Osaka, Japan; and [3]Lowe Center for Thoracic Oncology and Department of Medical Oncology, Dana-Farber Cancer Institute, Boston, Massachusetts

Note: Supplementary data for this article are available at Clinical Cancer Research Online (http://clincancerres.aacrjournals.org/).

Corresponding Author: Isamu Okamoto, Department of Medical Oncology, Kinki University Faculty of Medicine, 377-2 Ohno-higashi, Osaka-Sayama, Osaka 589-8511, Japan. Phone: 81-72-366-0221; Fax: 81-72-360-5000; E-mail: chi-okamoto@dotd.med.kindai.ac.jp

doi: 10.1158/1078-0432.CCR-10-2798

Published OnlineFirst March 17, 2011; DOI:10.1158/1078-0432.CCR-10-2798

Translational Relevance

EML4-ALK (echinoderm microtubule-associated protein–like 4 anaplastic lymphoma kinase) was recently identified as a transforming fusion gene in non–small cell lung cancer (NSCLC), and several selective inhibitors of the kinase activity of ALK, such as crizotinib, are currently undergoing clinical trials for the treatment of EML4-ALK–positive NSCLC. Identification of the signaling pathways responsible for malignant transformation by EML4-ALK will likely enhance further development of ALK-targeted therapy for NSCLC patients. We have now shown that both ERK (extracellular signal–regulated kinase) and STAT3 pathways are the principal mediators of EML4-ALK signaling, and we further identified the mediators of apoptosis induced by ALK inhibition. Our preclinical data provide both insight into the pathogenesis of EML4-ALK–positive lung cancer and a potential basis for the development of biomarkers for the efficacy of ALK-targeted therapy in patients with this condition.

EML4 portion, which confers marked transforming activity both *in vitro* and *in vivo* (4, 15).

ALK inhibitors have been found to suppress the growth of and to induce apoptosis in EML4-ALK–positive lung cancer cells, suggesting that ALK inhibition is a potential strategy for the treatment of NSCLC patients with this molecular abnormality (9, 16). Indeed, a selective inhibitor of the kinase activity of ALK, crizotinib, is currently undergoing clinical trials and has shown high efficacy in NSCLC patients with EML4-ALK (17). However, the downstream signaling pathways that regulate the proliferation or survival of EML4-ALK–positive lung cancer cells have remained to be well established, and the key mediators of ALK inhibitor–induced apoptosis have not been fully determined. In the present study, we constructed expression vectors for EML4-ALK variants 1 and 3 and then established cells stably expressing these proteins. With the use of these cells, we examined the signaling molecules that function downstream of EML4-ALK. We further investigated the molecular mechanisms underlying ALK inhibitor–induced apoptosis in EML4-ALK–positive lung cancer cells.

Materials and Methods

Cell culture and reagents

NIH 3T3 cells as well as the human cancer cell lines H2228 and Karpas299 were obtained from American Type Culture Collection. H3122 cells were obtained as previously described (9). NIH 3T3 cells were cultured in Dulbecco's modified Eagle's medium (Sigma) supplemented with 10% FBS and 1% penicillin-streptomycin. H2228, Karpas299, and H3122 cells were cultured in RPMI 1640 medium (Sigma) supplemented with 10% FBS and 1% penicillin-streptomycin. All cells were maintained under a humidified atmosphere of 5% CO_2 at 37°C. U0126 and LY294002 were obtained from Cell Signaling Technology and TAE684 was from ShangHai Biochempartner.

Cell transfection

A cDNA for EML4-ALK variant 1 was cloned into pDNR-Dual (Becton Dickinson) as previously described (9). A full-length cDNA fragment encoding EML4-ALK variant 3b was obtained from H2228 cells by reverse transcription and the PCR with the primers EAV-F (5′-AAGCTTCGCAAGATGGACGGTTTCGCCGGCAGTC-3′) and EAV-R (5′-GCGGCCGCTCAGGGCCCAGGC-TGGTTCATGCT-3′). Amplification products were verified by sequencing after their cloning into the pCR-Blunt II-TOPO vector (Invitrogen). The EML4-ALK variant 1 or 3b cDNA was excised from pCR-Blunt II-TOPO and transferred to either pcDNA3.1-Hygro(+) (Invitrogen) or pMZs (Cell Biolabs). A pBabe-puro vector encoding CA-STAT3 with a COOH-terminal FLAG tag was kindly provided by J. Bromberg (18). A pQCXIH-survivin vector was constructed as previously described (19). All expression vectors were introduced into NIH 3T3 cells as previously described (20, 21).

Immunoblot analysis

Cells were washed twice with ice-cold PBS and then lysed in a solution containing 20 mmol/L Tris-HCl (pH 7.5), 150 mmol/L NaCl, 1 mmol/L EDTA, 1% Triton X-100, 2.5 mmol/L sodium pyrophosphate, 1 mmol/L phenylmethylsulfonyl fluoride, and leupeptin (1 μg/mL). The protein concentration of cell lysates was determined with the Bradford reagent (Bio-Rad), and equal amounts of protein were subjected to SDS-PAGE on a 7.5% or 12% gel. The separated proteins were transferred to a nitrocellulose membrane, which was then exposed to 5% nonfat dried milk in PBS for 1 hour at room temperature before incubation overnight at 4°C with primary antibodies. Rabbit polyclonal antibodies to human phosphorylated ALK (pY1608), to ALK, to phosphorylated extracellular signal–regulated kinase (ERK), to ERK, to phosphorylated STAT3, to STAT3, to phosphorylated AKT, to AKT, to PARP, to BIM, to Mcl-1, to Bcl-xL, to X-linked inhibitor of apoptosis (XIAP), and to FLAG were obtained from Cell Signaling Technology; those to survivin were from Novos; and those to β-actin were from Sigma. All antibodies were used at a 1:1,000 dilution, with the exception of those to β-actin (1:200). The membrane was then washed with PBS containing 0.05% Tween 20 before incubation for 1 hour at room temperature with horseradish peroxidase–conjugated goat antibodies to rabbit IgG (Sigma). Immune complexes were finally detected with chemiluminescence reagents (GE Healthcare).

Cell growth inhibition assay

Cells were plated in 96-well, flat-bottomed plates and cultured for 24 hours before exposure to various concentrations of drugs for 72 hours. TetraColor One (5 mmol/L tetrazolium monosodium salt and 0.2 mmol/L 1-methoxy-5-methyl phenazinium methylsulfate; Seikagaku) was then